Computational Mechanics 14 (1994) 549–585 © Springer-Verlag 1994

Analysis of strain localization in strain-softening hyperelastic materials, using assumed stress hybrid elements

W. Seki, S. N. Atluri

Abstract Newly developed assumed stress finite elements, based on a mixed variational principle which includes unsymmetric stress, rotation (drilling degrees of freedom), pressure, and displacement as variables, are presented. The elements are capable of handling geometrically nonlinear as well as materially nonlinear two dimensional problems, with and without volume constraints. As an application of the elements, strain localization problems are investigated in incompressible materials which have strain softening elastic constitutive relations. It is found that the arclength method, in conjunction with the Newton Raphson procedure, plays a crucial role in dealing with problems of this kind to pass through the limit load and bifurcation points in the solution paths. The numerical examples demonstrate that the present numerical procedures capture the formation of shear bands successfully and the results are in good agreement with analytical solutions.

List of Symbols

$\mathbf{u}$	displacement
$\mathbf{R}$	rotation
$\mathbf{U}$	right stretch tensor
$\mathbf{r}^*$	Biot stresss tensor
$\mathbf{t}$	first Piola Kirchhoff stress tensor
τ	Cauchy stress tensor
$\mathbf{I}$	identity tensor
$\mathbf{F}$	deformation gradient $:= \mathbf{I} + (\nabla \mathbf{u})^T$
$\mathbf{ab}$	$:= a_i b_j \mathbf{g}^i \mathbf{g}^j$ = dyad
$\mathbf{a}\cdot\mathbf{b}$	$:= a_i b^i$ = dot product
$\mathbf{A}\cdot\mathbf{b}$	$:= A_{ij} b^j \mathbf{g}^i$
$\mathbf{A}\cdot\mathbf{B}$	$:= A_{ik} B^k{}_j \mathbf{g}^i \mathbf{g}^j$
$\mathbf{A}:\mathbf{B}$	$:= A_{ij} B^{ij}$
$\mathbf{v}$	velocity $:= \dot{\mathbf{u}}$
$\mathbf{W}$	spin tensor $:= \dot{\mathbf{R}}$
$\mathbf{D}$	rate of stretch $:= \dot{\mathbf{U}}$
$\dot{\mathbf{r}}^*$	UL rate of $\mathbf{r}^*$
$\dot{\mathbf{t}}$	UL rate of $\mathbf{t}$
δ_{ij}	Kronecker's delta
∇	$:= \mathbf{g}_i \frac{\partial}{\partial \xi_i}$
J	$:= \det \mathbf{F} = \det\{\mathbf{I} + (\nabla \mathbf{u})^T\}$
symm (A)	$:= \frac{1}{2}(\mathbf{A} + \mathbf{A}^T)$
skew (A)	$:= \frac{1}{2}(\mathbf{A} - \mathbf{A}^T)$
trace (A)	$:= A^r_{\ r}$

Communicated by S. N. Atluri, 30 March 1994

Computational Mechanics Center, Georgia Institute of Technology, Atlanta, Georgia 30332-0356

This research is supported by the Office of Naval Research. The first author wishes to express his appreciation to Dr. H. Murakawa, Dr. E. F. Punch, Mr. A. Cazzani, and Dr. H. Okada for fruitful discussions on the subject

$|\mathbf{a}|^2 := \mathbf{a}\cdot\mathbf{a} = a_i a^i$
$|\mathbf{A}|^2 := \mathbf{A}:\mathbf{A} = A_{ij}A^{ij}$
where **a**, **b**; vectors, **A**, **B**; tensors (second order), $\mathbf{A}^T$; transpose of **A**, ($\mathbf{g}_i$); base vectors.

1 Introduction

The purposes of this research are primarily, to present new assumed stress hybrid elements with drilling degrees of freedom, with and without volume constraints, for the analysis of large deformation problems, and secondarily, to investigate applicability of the elements for analyzing shear localization problems in strain softening hyperelastic materials.

The assumed stress hybrid elements, based on the complementary energy variational principle, were pioneered by Pian (1964) for linear elasticity. The formulations of the assumed stress hybrid elements for nonlinear problems were presented by Atluri (1973), Atluri and Murakawa (1977), and by Murakawa and Atluri (1978, 1979) using mixed variational principles with and without volume constraints. Although the earlier formulations of assumed stress hybrid elements suffered certain deficiencies (e.g. kinematic or spurious modes, coordinate invariance, stability etc.), several significant contributions have appeared to establish robust assumed stress hybrid element formulations. See Pian and Sumihara (1984), Xue et al. (1983), Punch and Atluri (1983), Rubinstein et al. (1983), Reed and Atluri (1983).

In the research on mixed formulations of finite elements methods, the elements with drilling degrees of freedom have attracted much attention recently for shell and membrane problems. The concept of these elements appeared first in the mid-'60s and was revived by Allman (1984). In the earlier works, however, the drilling degrees of freedom were not treated as independent fields and the efforts were mostly unsuccessful. The variational formulation with a so-called regularization term, proposed by Hughes and Brezzi (1990), makes it possible to utilize complementary-energy based variational principles to construct robust mixed element formulations with drilling degrees of freedom. For geometrically linear problems, Cazzani and Atluri (1993) presented a quadrilateral membrane element with a drilling degree of freedom, unsymmetric stress, and displacement as independent fields. The excellent performance of the elements was thoroughly examined (see also Iura and Atluri 1992) and the present work may be thought of as a generalization of these elements for nonlinear problems.

The applications of finite elements for shear localization problems has been extensively studied during the last decade. However, it is observed that shear bands captured by ordinary displacement-type finite elements are mostly mesh-dependent because the width of shear bands is usually much smaller than the available element size. Several approaches to overcome these difficulties in displacement-type finite elements have appeared so far: for example, the introduction of the embedded localized strain fields (Ortiz et al. 1987; Belytschki et al. 1988), adaptive mesh method (Batra and Ko 1992), etc.

In this paper, the assumed stress hybrid elements, recently developed by the authors, are presented and applied to the solution of the shear localization problems. These elements are quite attractive because: (i) the shear band emerges as a natural solution of a boundary value problem without resorting to bifurcation analysis at each element level: (ii) the elements are free of locking under incompressible deformation through the use of multiplicative decomposition of the distortional and the volumetric strain fields. Four noded quadrilateral shaped plane stress and plane strain elements are developed, based on the discretized forms of the mixed variational principles with deviatoric parts of unsymmetric stress (Biot stress), hydrostatic pressure, displacement, and drilling degree of freedom as independent fields.

The material properties treated in this paper are rate-independent hyperelastic types, though the developed methodology is also applicable to elastic-plastic problems. The strain softening type constitutive relations are specified through strain energy functions with a small number of material parameters. The development of shear localization is triggered only by the characteristic of the constitutive relations, and no further threshold conditions are involved.

The arclength method (Riks 1972; Chrisfield 1983; Kondoh and Atluri 1985) is used to solve the snap-through and bifurcation phenomena which are encountered in dealing with elastically unstable problems. It is found that the use of this method in conjunction with the Newton-Raphson procedure is crucially important, since in most of the cases, there are limit loads and/or limit displacements in the global mechanical response of the body, and a simple load- or displacement-control method cannot follow the solution path. Numerical examples demonstrate that the elements successfully capture the shear bands and the results are in good agreement with the analytical solutions.

The contents of the paper are as follows. In Sect. 2, the basic variational principles, the multiplicative decomposition of the deformation, rate forms, and the regularizations of the principles are discussed. In Sect. 3, the appropriate discretizations of the principles and the numerical strategy are presented. Some benchmark test results are also given in this section. In Sect. 4, numerical examples of shear localization problems are presented and discussed.

2
Variational principles for finite deformation

We start with a discussion of the basic variational principles of continuum mechanics to construct finite element formulations for nonlinear problems.

In this section, we choose the suitable forms of variational principles from several possible forms, using alternative stress and conjugate strain measures as shown by Atluri (1984). In this research, we adopt the forms using an unsymmetric stress as the stress measure. For practical numerical implementation, strain fields are eliminated in the mixed variational principles, leading to a finite element stiffness approach.

The second step is the decomposition of distortional and dilatational portion of the deformation fields. In this paper, due to the necessity of dealing with finite strains, we choose the principles with multiplicative decomposition of deformation, as derived by Atluri and Reissner (1989).

As a third step, we derive the rate forms of the variational principles for the time integration of the derived initial value problems. We focus on the Update Lagrangean rate forms to deal with hyperelastic as well as elastic-plastic materials.

In the fourth step, we suggest the regularization of the variational principles for large deformation problems. Since the strain energy density function depends on only the symmetric part of the strain, it is not possible to eliminate the stress fields at element level using the complementary energy function in the context of finite element formulation. For linear elasticity, Hughes and Brezzi (1989) proposed to modify the variational principle. Through a regularization term in order to make the complementary energy function be quadratic in terms of the skew parts of the stress components. Since this process is quite important for finite element formulation, especially for shell or membrane problems, several regularization forms are proposed and discussed.

2.1
Variational principle using unsymmetric (Piola or Biot) stress

It is well known that every field equation and boundary condition of a boundary value problem of an elastic body can be derived from the stationary condition of a general variational functional (Washizu 1982). For discussing the mechanics of a finitely deformed body, we adopt the Lagrangean description which uses the coordinate system fixed to the body at C_0 state. (C_0 state may or may not be the undeformed state.) The kinematics of the body are described, based on that coordinate system. We assume the existence of the strain energy W_0 as a function of right stretch tensor U. The four field mixed variational principle which includes the displacement $\mathbf{u}$, the right stretch tensor U, the unsymmetric Biot stress tensor $\mathbf{r}^*$, and the rotation R as variables, is written as follows (Atluri 1984).

$$F_1(\mathbf{u}, \mathbf{U}, \mathbf{R}, \mathbf{r}^*) = \int_{V_0} \{ W_0(\mathbf{U}) + \mathbf{r}^{*T} : [\mathbf{R}^T \cdot (\mathbf{I} + \nabla_0 \mathbf{u})^T - \mathbf{U}] - \rho_0 \mathbf{b} \cdot \mathbf{u} \}\, dv + [\text{Surface Integral}] \tag{1}$$

where

$$[\text{Surface Integral}] = -\int_{S_{\sigma 0}} \bar{\mathbf{T}} \cdot \mathbf{u}\, ds - \int_{S_{u0}} (\mathbf{t}^T \cdot \mathbf{n}) \cdot (\mathbf{u} - \bar{\mathbf{u}})\, ds \tag{2}$$

and V_0, ρ_0 are respectively the volume and density of the body at C_0; $\mathbf{b}$ is the body force; $\mathbf{t}$ is the first Piola Kirchhoff stress tensor ($\mathbf{t} = \mathbf{r}^* \cdot \mathbf{R}^T$); $\mathbf{n}$ is the normal vector of the surface; $S_{\sigma 0}$ is the surface of the body at C_0 on which the load vector $\bar{\mathbf{T}}$ is applied; S_{u0} is the surface on which the displacement $\bar{\mathbf{u}}$ is prescribed.

Note that, as the a priori conditions, we require the symmetry of $\mathbf{U}$ ($\mathbf{U}^T = \mathbf{U}$) and the orthogonality of $\mathbf{R}$ ($\mathbf{R}^T \cdot \mathbf{R} = \mathbf{I}$).

It may be instructive to derive the Euler equations corresponding to the stationary of F_1 by taking a variation.

$$\begin{aligned} \delta F_1(\mathbf{u}, \mathbf{U}, \mathbf{R}, \mathbf{r}^*) = \int_{V_0} \Bigg\{ & \left[\frac{\partial W_0(\mathbf{U})}{\partial \mathbf{U}} - \operatorname{symm} \mathbf{r}^* \right] : \delta \mathbf{U} + [\mathbf{R}^T \cdot (\mathbf{I} + \nabla_0 \mathbf{u})^T - \mathbf{U}] : \delta \mathbf{r}^{*T} \\ & + [\mathbf{R}^T \cdot (\mathbf{I} + \nabla_0 \mathbf{u})^T \cdot \mathbf{r}^*] : [\mathbf{R}^T \cdot \delta \mathbf{R}] - [\nabla_0 \cdot (\mathbf{r}^* \cdot \mathbf{R}^T) + \rho_0 \mathbf{b}] \cdot \delta \mathbf{u} \Bigg\}\, dv \\ & + \delta [\text{Surface Integral}] \end{aligned} \tag{3}$$

where

$$\delta [\text{Surface Integral}] = -\int_{S_{\sigma 0}} (\mathbf{t}^T \cdot \mathbf{n} - \bar{\mathbf{T}}) \cdot \delta \mathbf{u}\, ds - \int_{S_{u0}} (\mathbf{u} - \bar{\mathbf{u}}) \cdot (\delta \mathbf{t}^T \cdot \mathbf{n})\, ds. \tag{4}$$

The stationary condition $\delta F_1 = 0$ gives following equations.

- Constitutive Relation (CR)

$$\frac{\partial W_0(\mathbf{U})}{\partial \mathbf{U}} - \text{symm}\,\mathbf{r}^* = 0. \tag{5}$$

- Compatibility Condition (CC)

$$\mathbf{R}^T\cdot(\mathbf{I} + \nabla_0\mathbf{u})^T - \mathbf{U} = 0. \tag{6}$$

- Linear Momentum Balance (LMB)

$$\nabla_0\cdot(\mathbf{r}^*\cdot\mathbf{R}^T) + \rho_0\mathbf{b} = 0. \tag{7}$$

- Angular Momentum Balance (AMB)

$$\mathbf{R}^T\cdot(\mathbf{I} + \nabla_0\mathbf{u})^T\cdot\mathbf{r}^* = \text{symmetric} \tag{8}$$

- Traction Boundary Condition (TBC)

$$\mathbf{t}^T\cdot\mathbf{n} - \bar{\mathbf{T}} = 0 \quad \text{on} \quad S_{\sigma 0}. \tag{9}$$

- Displacement Boundary Condition (DBC)

$$\mathbf{u} - \bar{\mathbf{u}} = 0 \quad \text{on} \quad S_{u0}. \tag{10}$$

Note that in AMB, we use the a priori condition that $\mathbf{R}^T\cdot\delta\mathbf{R}$ = skew symmetric.

The compatibility condition $(\mathbf{I} + \nabla^0\mathbf{u})^T = \mathbf{F} = \mathbf{R}\cdot\mathbf{U}$ is often referred to as the polar decomposition of the deformation gradient **F**.

For deriving TBC, we use the Gauss' divergence theorem:

$$\int_{V_0} \mathbf{t}:(\nabla_0\,\delta\mathbf{u})\,dv = \int_{V_0} -(\nabla_0\cdot\mathbf{t})\cdot\delta\mathbf{u}\,dv + \int_{S_0} -(\mathbf{t}^T\cdot\mathbf{n})\cdot\delta\mathbf{u}\,ds. \tag{11}$$

Now, for practical finite element implementation, it is preferable to eliminate the stretch **U**. One way to do this, is to choose for **U** (which is required to be symmetric a priori) not an indepedent field, but to write it in terms of the independently chosen fields **u** and **R**, as:

$$\mathbf{U} = \text{symm}\,[\mathbf{R}^T\cdot(\mathbf{I} + \nabla_0\mathbf{u})^T] \tag{12}$$

then we have a three field principle with **u**, **R**, and skew$(\mathbf{r}^*)$ as variables. One may also obtain a principle with only kinematic fields, by eliminating skew$(\mathbf{r}^*)$ to construct displacement type elements.

However, in this research, we take the opposite approach. Through the contact transformation:

$$-W_c(\text{symm}\,\mathbf{r}^*) = W_0(\mathbf{U}) - \mathbf{U}:\mathbf{r}^{*T} = W_0(\mathbf{U}) - \mathbf{U}:(\text{symm}\,\mathbf{r}^*). \tag{13}$$

We have the following functional, as a basis for a three field mixed principle.

$$F_2(\mathbf{u},\mathbf{R},\mathbf{r}^*) = \int_{V_0}\{-W_c(\text{symm}\,\mathbf{r}^*) + \mathbf{r}^{*T}:[\mathbf{R}^T\cdot(\mathbf{I} + \nabla_0\mathbf{u})^T] - \rho_0\mathbf{b}\cdot\mathbf{u}\}\,dv + [\text{Surface Integral}]. \tag{14}$$

In this form, the symmetry of $\mathbf{U} = \mathbf{R}^T\cdot(\mathbf{I} + \nabla_0\mathbf{u})^T$ is enforced through the Euler equation:

$$\frac{\partial W_c(\text{symm}\,\mathbf{r}^*)}{\partial(\mathbf{r}^*)^T} = \mathbf{R}^T\cdot(\mathbf{I} + \nabla_0\mathbf{u})^T = \text{symmetric}. \tag{15}$$

Murakawa and Atluri (1978) and Reed and Atluri (1982) constructed finite elements based on the principle using the first Piola Krichhoff stress tensor **t**. This form can be derived using (1) and

$\mathbf{t} = \mathbf{r}^* \cdot \mathbf{R}^T$ as follows.

$$F_2(\mathbf{u}, \mathbf{U}, \mathbf{R}, \mathbf{t}) = \int_{V_0} \{ W_0(\mathbf{U}) + \mathbf{t}^T : [(\mathbf{I} + \nabla_0 \mathbf{u})^T - \mathbf{R} \cdot \mathbf{U}] - \rho_0 \mathbf{b} \cdot \mathbf{u} \} \, dv + [\text{Surface Integral}]. \tag{16}$$

Theoretically, the principles (1) and (16) are almost equivalent and both of them are applicable for nonlinear problems. From the practical point of view, the notation can be slightly simplified to treat nonlinear constitutive laws by using the Biot stress tensors, so we adopt the previous form (1) in this research.

2.2 Multiplicative decomposition

To deal with problems of incompressible materials, it is often convenient to separate dilatational parts from distortional parts in the deformation field. For nonlinear problems, it can be done through multiplicative decomposition. We introduce the new fields $\mathbf{U}'$ and J defined as:

$$J = \det \mathbf{U}$$

$$\mathbf{U}' = \mathbf{U} J^{-1/3}. \tag{17}$$

The strain energy function $W_0(\mathbf{U})$ will be given in terms of the now independent fields $\mathbf{U}'$ and J as:

$$W_0(\mathbf{U}) = W_0(\mathbf{U}' J^{1/3}) = W_0'(\mathbf{U}', J). \tag{18}$$

We also need to decompose stress field $\mathbf{r}^*$ to $(\mathbf{r}^{*'}, p)$ corresponding to $(\mathbf{U}', J)$. Then, the principle (1) can be rewritten as the following 6-field principle (Atluri and Reissner 1989).

$$G_1(\mathbf{u}, \mathbf{U}', J, \mathbf{R}, \mathbf{r}^{*'}, p) = \int_{V_0} \{ W_0'(\mathbf{U}', J) + \mathbf{r}^{*'T} : [\mathbf{R}^T \cdot (\mathbf{I} + \nabla_0 \mathbf{u})^T J_{\mathbf{u},\mathbf{R}}^{-1/3} - \mathbf{U}'] + [f(J_{\mathbf{u},\mathbf{R}}) - f(J)] p - \rho_0 \mathbf{b} \cdot \mathbf{u} \} \, dv + [\text{Surface Integral}] \tag{19}$$

where we use the following 'dummy' variable (which depends on $\mathbf{u}$, $\mathbf{R}$) for ease of exposition:

$$J_{\mathbf{u},\mathbf{R}} = \det \{ \text{symm} [\mathbf{R}^T \cdot (\mathbf{I} + \nabla_0 \mathbf{u})^T \} \tag{20}$$

and f is smooth and monotone ($f' \neq 0$) function. If we choose $f(J) = J - 1$, p has the physical meaning of hydrostatic pressure.

Again, by taking the variation of G_1,

$$\begin{aligned} \delta G_1(\mathbf{u}, \mathbf{U}', J, \mathbf{R}, \mathbf{r}^{*'}, p) = \int_{V_0} \Bigg\{ & \left[\frac{\partial W_0'(\mathbf{U}', J)}{\partial \mathbf{U}'} - \text{symm}\, \mathbf{r}^{*'} \right] : \delta \mathbf{U}' + \left[\frac{\partial W_0'(\mathbf{U}', J)}{\partial J} - f'(J) p \right] \delta J \\ & + [\mathbf{R}^T \cdot (\mathbf{I} + \nabla_0 \mathbf{u})^T J_{\mathbf{u},\mathbf{R}}^{-1/3} - \mathbf{U}'] : \delta \mathbf{r}^{*'T} + [f(J_{\mathbf{u},\mathbf{R}}) - f(J)] \, \delta p \\ & + [\mathbf{R}^T \cdot (\mathbf{I} + \nabla_0 \mathbf{u})^T \cdot \mathbf{r}^{*'} J_{\mathbf{u},\mathbf{R}}^{-1/3} \\ & - \frac{1}{3} [\mathbf{r}^* : \{ (\mathbf{I} + \nabla_0 \mathbf{u}) \cdot \mathbf{R} \} J_{\mathbf{u},\mathbf{R}}^{-1/3}] \mathbf{R}^T \cdot (\mathbf{I} + \nabla_0 \mathbf{u})^T \cdot \hat{\mathbf{U}}^{-1} \\ & + p f'(J_{\mathbf{u},\mathbf{R}}) J_{\mathbf{u},\mathbf{R}} \mathbf{R}^T \cdot (\mathbf{I} + \nabla_0 \mathbf{u})^T \cdot \hat{\mathbf{U}}^{-1}] : [\mathbf{R}^T \cdot \delta \mathbf{R}] \\ & - [\nabla_0 \cdot \{ \mathbf{r}^{*'} \cdot \mathbf{R}^T J_{\mathbf{u},\mathbf{R}}^{-1/3} - \frac{1}{3} [\mathbf{r}^{*'} : \{ (\mathbf{I} + \nabla_0 \mathbf{u}) \cdot \mathbf{R} \} J_{\mathbf{u},\mathbf{R}}^{-1/3}] \hat{\mathbf{U}}^{-1} \cdot \mathbf{R}^T \\ & + p f'(J_{\mathbf{u},\mathbf{R}}) J_{\mathbf{u},\mathbf{R}} \hat{\mathbf{U}}^{-1} \cdot \mathbf{R}^T \} + \rho_0 \mathbf{b}] \cdot \delta \mathbf{u} \Bigg\} dv \\ & + \delta [\text{Surfce Integral}] \end{aligned} \tag{21}$$

where $\hat{\mathbf{U}} = \text{symm} [\mathbf{R}^T \cdot (\mathbf{I} + \nabla_0 \mathbf{u})^T]$.

Then, we have the following Euler equations.

- Constitutive Relation (CR)

$$\frac{\partial W_0'(\mathbf{U}', J)}{\partial \mathbf{U}'} - \text{symm}\, \mathbf{r}^{\star'} = 0$$

$$\frac{\partial W_0'(\mathbf{U}', J)}{\partial J} - f'(J)p = 0. \tag{22}$$

- Compatibility Condition (CC)

$$\mathbf{R}^T \cdot (\mathbf{I} + \nabla_0 \mathbf{u})^T J_{\mathrm{u,R}}^{-1/3} - \mathbf{U}' = 0$$

$$J_{\mathrm{u,R}} - J = 0. \tag{23}$$

- Linear Momentum Balance (LMB)

$$\nabla_0 \cdot \left\{ \mathbf{r}^{\star'} \cdot \mathbf{R}^T J_{\mathrm{u,R}}^{-1/3} - \frac{1}{3} [\mathbf{r}^{\star'} : \{(\mathbf{I} + \nabla_0 \mathbf{u}) \cdot \mathbf{R}\} J_{\mathrm{u,R}}^{-1/3}] \hat{\mathbf{U}}^{-1} \cdot \mathbf{R}^T + p f'(J_{\mathrm{u,R}}) J_{\mathrm{u,R}} \hat{\mathbf{U}}^{-1} \cdot \mathbf{R}^T \right\} + \rho_0 \mathbf{b} = 0 \tag{24}$$

- Angular Momentum Balance (AMB)

$$\mathbf{R}^T \cdot (\mathbf{I} + \nabla_0 \mathbf{u})^T \cdot \mathbf{r}^{\star'} - \frac{1}{3} [\mathbf{r}^{\star'} : \{(\mathbf{I} + \nabla_0 \mathbf{u}) \cdot \mathbf{R}\} J_{\mathrm{u,R}}^{-1/3}] \mathbf{R}^T \cdot (\mathbf{I} + \nabla_0 \mathbf{u})^T \cdot \hat{\mathbf{U}}^{-1}$$

$$+ p f'(J_{\mathrm{u,R}}) J_{\mathrm{u,R}} \mathbf{R}^T \cdot (\mathbf{I} + \nabla_0 \mathbf{u})^T \cdot \hat{\mathbf{U}}^{-1} = \text{symmetric} \tag{25}$$

TBC, DBC are the same as before.

To see that LMB, AMB, and TBC are expected ones, we note that the stationary condition gives:

$$\mathbf{R}^T \cdot (\mathbf{I} + \nabla_0 \mathbf{u})^T = \text{symmetic} = \hat{\mathbf{U}} = \mathbf{U}$$

so

$$\hat{\mathbf{U}}^{-1} \cdot \mathbf{R}^T = [(\mathbf{I} + \nabla_0 \mathbf{u})^T]^{-1} = (\mathbf{I} + \nabla_0 \mathbf{u})^T \tag{26}$$

and by using the relation:

$$\mathbf{t} = \mathbf{r}^{\star} \cdot \mathbf{R}^T$$

$$= \mathbf{r}^{\star'} \cdot \mathbf{R}^T J^{-1/3} - \frac{1}{3} [\mathbf{r}^{\star'} : \{(\mathbf{I} + \nabla_0 \mathbf{u}) \cdot \mathbf{R}\} J^{-1/3}] (\mathbf{I} + \nabla_0 \mathbf{u})^{-T} + p f'(J) J (\mathbf{I} + \nabla_0 \mathbf{u})^{-T} \tag{27}$$

one may find that LMB, AMB, and TBC are equivalent as before (7) ~ (9).

Now, a four field mixed variational principle can be achieved through the contact transformation:

$$-W_c'(\text{symm}\, \mathbf{r}^{\star'}, p) = W_0'(\mathbf{U}', J) - \mathbf{U}' : \text{symm}\, \mathbf{r}^{\star'} - p f(J). \tag{28}$$

Thus, we have the four field principle, with the associated functional:

$$G_2(\mathbf{u}, \mathbf{R}, \mathbf{r}^{\star'}, p) = \int_{V_0} \{ W_c'(\text{symm}\, \mathbf{r}^{\star'}, p) + \mathbf{r}^{\star' T} : [\mathbf{R}^T \cdot (\mathbf{I} + \nabla_0 \mathbf{u})^T J_{\mathrm{u,R}}^{-1/3}]$$

$$+ f(J_{\mathrm{u,R}}) p - \rho_0 \mathbf{b} \cdot \mathbf{u} \} \, dv$$

$$+ [\text{Surface Integral}]. \tag{29}$$

Now, the constitutive relations are separated into distortional and volumetric parts as follows:

$$\frac{\partial W_c'(\text{symm}\,\mathbf{r}^{*'}, p)}{\partial (\mathbf{r}^{*'})^T} = \mathbf{R}^T \cdot (\mathbf{I} + \nabla_0 \mathbf{u})^T J_{\mathrm{u.R}}^{-1/3} = \text{symmetric}$$

$$\frac{\partial W_c'(\text{symm}\,\mathbf{r}^{*'}, p)}{\partial p} = f(J_{\mathrm{u.R}}). \tag{30}$$

The decomposed forms (19) and (29) are applicable for both compressible and incompressible materials. Perfect incompressibility is imposed through W_0:

$$\frac{\partial W_c'(\mathbf{U}', J)}{\partial J} = \text{bulk modulus} = \infty \tag{31}$$

or through W_c:

$$\frac{\partial W_c'(\text{symm}\,\mathbf{r}^{*'}, p)}{\partial p} = \text{bulk compliance} = 0. \tag{32}$$

2.3 Rate principles

In order to develop continuation methods to solve nonlinear problems, it is often convenient to consistently 'linearize' the variational principles into their rate forms. In solid mechanics, the Total Lagrangean (TL) and Update Lagrangean (UL) forms are widely used. The TL rate form refers to the initial or undeformed configuration of the body C_0, whereas the UL rate refers to the configuration at the previous incremental step C_N. Usually, the UL form is preferred for hyperelastic and elastic-plastic problems due to its simplicity. Here, we discuss the rate forms using the Update Lagrangean (UL) descritpion only. For a discussion of TL forms, see Atluri (1977, 1980). The UL rate of a physical quantity x is denoted as $\dot{x}$. For brevity, we also use the following notations.

$$\dot{\mathbf{u}} = \mathbf{v}, \quad \dot{\mathbf{U}} = \mathbf{D}, \quad \dot{\mathbf{R}} = \mathbf{W}. \tag{33}$$

It is well-known that $\mathbf{D}^T = \mathbf{D}$ and $\mathbf{W}^T = -\mathbf{W}$.

Once again, we start from the four field principle for consistency and ease of manipulation. The rate form of the principle F_1, given by Atluri (1980), is as follows.

$$\begin{aligned}\dot{F}_1(\mathbf{v}, \mathbf{D}, \mathbf{W}, \dot{\mathbf{r}}^*) = \int_{V_N} \Big\{ & \dot{W}(\mathbf{D}) - \frac{1}{2}\tau^N : (\mathbf{W}\cdot\mathbf{W}^T) + \tau^{NT} : [\mathbf{W}^T \cdot (\nabla^N \mathbf{v})^T] \\ & + \dot{\mathbf{r}}^{*T} : [(\nabla^N \mathbf{v})^T - \mathbf{D} - \mathbf{W}] - \rho^N \dot{\mathbf{b}} \cdot \mathbf{v} \Big\} dv \\ & + \dot{\overline{[\text{Surface Integral}]}}\end{aligned} \tag{34}$$

where

$$\dot{\overline{[\text{Surface Integral}]}} = -\int_{S_{\sigma N}} \dot{\bar{\mathbf{T}}} \cdot \mathbf{v}\, ds - \int_{S_{uN}} (\dot{\mathbf{t}}^T \cdot \mathbf{n}) \cdot (\mathbf{v} - \bar{\mathbf{v}})\, ds \tag{35}$$

τ^N is the Cauchy (true) stress tensor and ρ^N is the density at the C_N state.

The rate forms of Euler equations are presented as follows.

- Constitutive Relation (CR)

$$\frac{\partial \dot{W}(\mathbf{D})}{\partial \mathbf{D}} - \text{symm}\,\dot{\mathbf{r}}^* = 0. \tag{36}$$

- Compatibility Condition (CC)

$$(\nabla^N \mathbf{v})^T - \mathbf{D} - \mathbf{W} = 0. \tag{37}$$

- Linear Momentum Balance (LMB)

$$\nabla^N\cdot(\dot{\mathbf{r}}^* - \tau^N\cdot\mathbf{W}) + \rho^N\dot{\mathbf{b}} = 0. \tag{38}$$

- Angular Momentum Balance (AMB)

$$\dot{\mathbf{r}}^* + [(\nabla^N\mathbf{v})^T - \mathbf{W}]\cdot\tau^N = \text{symmetric}. \tag{39}$$

- Traction Boundary Condition (TBC)

$$\dot{\mathbf{t}}^T\cdot\mathbf{n} - \dot{\bar{\mathbf{T}}} = 0 \quad \text{on} \quad S_{\sigma N} \tag{40}$$

- Displacement Boundary Condition (DBC)

$$\mathbf{v} - \bar{\mathbf{v}} = 0 \quad \text{on} \quad S_{uN} \tag{41}$$

The rate form of the 6-field theory (G_1) is given as:

$$\begin{aligned}\dot{G}_1(\mathbf{v},\mathbf{D}',\dot{J},\mathbf{W},\dot{\mathbf{r}}^{*'},\dot{p}) = \int_{V_N}\Big\{ &\dot{W}'(\mathbf{D}',\dot{J}) - \frac{1}{2}\tau^N{:}(\mathbf{W}\cdot\mathbf{W}^T) + \tau^{NT}{:}[\mathbf{W}^T\cdot(\nabla^N\mathbf{v})^T] \\ &+ \dot{\mathbf{r}}^{*'T}{:}\left[(\nabla^N\mathbf{v})^T - \mathbf{D}' - \mathbf{W} - \frac{1}{3}\operatorname{trace}(\nabla^N\mathbf{v})\mathbf{I}\right] \\ &+ \left[\operatorname{trace}(\nabla^N\mathbf{v}) - \dot{J}\right]\dot{p} - \rho^N\dot{\mathbf{b}}\cdot\mathbf{v}\Big\}\,dv \\ &+ \dot{\overline{[\text{Surface Integral}]}}\end{aligned} \tag{42}$$

where we choose $f(J) = J - 1$.

Note that:

$$\dot{J}_{\mathrm{u,R}} = \operatorname{trace}(\nabla^N\mathbf{v}). \tag{43}$$

So, the multiplicative decomposition results in a similar form of additive decomposition in its UL rate from.

The Euler equations are shown below:

- Constitutive Relation (CR)

$$\frac{\partial\dot{W}'(\mathbf{D}',\dot{J})}{\partial\mathbf{D}'} - \operatorname{symm}\dot{\mathbf{r}}^{*'} = 0$$

$$\frac{\partial\dot{W}'(\mathbf{D}',\dot{J})}{\partial\dot{J}} - \dot{p} = 0. \tag{44}$$

- Compatibility Condition (CC)

$$(\nabla^N\mathbf{v})^T - \mathbf{D}' - \mathbf{W} - \frac{1}{3}\operatorname{trace}(\nabla^N\mathbf{v})\mathbf{I} = 0$$

$$\operatorname{trace}(\nabla^N\mathbf{v}) - \dot{J} = 0. \tag{45}$$

- Linear Momentum Balance (LMB)

$$\nabla^N\cdot\left(\dot{\mathbf{r}}^{*'} - \frac{1}{3}\operatorname{trace}(\dot{\mathbf{r}}^{*'})\mathbf{I} + \dot{p}\mathbf{I} - \tau^N\cdot\mathbf{W}\right) + \rho^N\dot{\mathbf{b}} = 0. \tag{46}$$

- Angular Momentum Balance (AMB)

$$\dot{\mathbf{r}}^{*'} + [(\nabla^N \mathbf{v})^T - \mathbf{W}] \cdot \tau^N = \text{symmetric} \tag{47}$$

TBC and DBC have the same forms as in the four field theory ($\dot{F}_1$). One may need the relation among $\dot{\mathbf{t}}$, $\dot{\mathbf{r}}^*$, and $\mathbf{W}$ to discern the TBC.

$$\dot{\mathbf{t}} = \dot{\mathbf{r}}^* - \tau^N \cdot \mathbf{W}$$

$$= \dot{\mathbf{r}}^{*'} - \frac{1}{3}\,\text{trace}(\dot{\mathbf{r}}^{*'})\mathbf{I} + \dot{p}\mathbf{I} - \tau^N \cdot \mathbf{W}. \tag{48}$$

By eliminating the stretch rate $\mathbf{D}$ from F_1, we have the rate form of F_2:

$$\dot{F}_2(\mathbf{v}, \mathbf{W}, \dot{\mathbf{r}}^*) = \int_{V_N} \Big\{ - \dot{W}_c(\text{symm}\,\dot{\mathbf{r}}^*) - \frac{1}{2}\,\tau^N : (\mathbf{W} \cdot \mathbf{W}^T) + \tau^{NT} : [\mathbf{W}^T \cdot (\nabla^N \mathbf{v})^T]$$

$$+ \dot{\mathbf{r}}^{*T} : [(\nabla^N \mathbf{v})^T - \mathbf{W}] - \rho^N \dot{\mathbf{b}} \cdot \mathbf{v} \Big\}\, dv$$

$$+ \dot{\overline{[\text{Surface Integral}]}} \tag{49}$$

where the contact transformation:

$$- \dot{W}_c(\text{symm}\,\dot{\mathbf{r}}^*) = \dot{W}'(\mathbf{D}) - \mathbf{D} : \text{symm}\,\dot{\mathbf{r}}^* \tag{50}$$

is used.

Likewise, by eliminating $\mathbf{D}'$ and $\dot{J}$ from G_1, we have the rate form of G_2:

$$\dot{G}_2(\mathbf{v}, \mathbf{W}, \dot{\mathbf{r}}^*, \dot{p}) = \int_{V_N} \Big\{ - \dot{W}'_c(\text{symm}\,\dot{\mathbf{r}}^*, \dot{p}) - \frac{1}{2}\,\tau^N : (\mathbf{W} \cdot \mathbf{W}^T) + \tau^{NT} : [\mathbf{W}^T \cdot (\nabla^N \mathbf{v})^T]$$

$$+ \dot{\mathbf{r}}^{*'T} : \left[(\nabla^N \mathbf{v})^T - \mathbf{W} - \frac{1}{3}\,\text{trace}(\nabla^N \mathbf{v})\mathbf{I} \right]$$

$$+ \text{trace}(\nabla^N \mathbf{v})\dot{p} - \rho^N \dot{\mathbf{b}} \cdot \mathbf{v} \Big\}\, dv$$

$$+ \dot{\overline{[\text{Surface Integral}]}} \tag{51}$$

where the contact transformation is:

$$- \dot{W}'_c(\text{symm}\,\dot{\mathbf{r}}^*, \dot{p}) = \dot{W}'(\mathbf{D}', \dot{J}) - \mathbf{D}' : \text{symm}\,\dot{\mathbf{r}}^{*'} - \dot{J}\dot{p}. \tag{52}$$

2.4
Regulation of the principles

In the three- and four-field mixed principles, (Eqs. (14), (29) and their rate forms in Eq. (49), (51) as well), the complementary energy W_c depends only the symmetric part of Biot stress $\mathbf{r}^*$. Hence, W_c is not positive definite in terms of $\mathbf{r}^*$ alone, and in the context of finite element formulation, it is not possible to eliminate every stress component at element level. This was a bottle-neck in constructing robust elements with drilling degrees of freedom. Hughes and Brezzi (1989) proposed to modify the following three field functional for linear elasticity:

$$\prod_1 (\mathbf{v}, \mathbf{W}, \boldsymbol{\sigma}) = \int_{V_0} \{ - W_c(\text{symm}\,\boldsymbol{\sigma}) + \boldsymbol{\sigma}^T : [(\nabla_0 \mathbf{v})^T - \mathbf{W}] - \rho_0 \mathbf{b} \cdot \mathbf{v} \}\, dv$$

$$+ [\text{Surface Integral}] \tag{53}$$

through a regularization given by:

$$\prod_{1\gamma}(\mathbf{v},\mathbf{W},\boldsymbol{\sigma}) = \prod_{1}(\mathbf{v},\mathbf{W},\boldsymbol{\sigma}) - \frac{1}{2\gamma}\int_{V_0} |\text{skew}\,\boldsymbol{\sigma}|^2\, dv \tag{54}$$

where γ is a positive constant. Here, $\boldsymbol{\sigma}$, the stress tensor for small deformation, is not assumed to be a priori symmetric (but is a posteriori symmetric). The regularized principle is positive definite in terms of $\boldsymbol{\sigma}$ because it is now quadratic in the skew part of $\boldsymbol{\sigma}$. Nevertheless, the regularized principle gives formally equivalent Euler equations. Therefore the process is quite important for numerical implementation of the elements with drilling degrees of freedom.

Cazzani and Atluri (1993) used the form:

$$F_2(\mathbf{v},\mathbf{W},\mathbf{t}) = \int_{V_0}\left\{ - W_c(\text{symm}\,\mathbf{t}) + \mathbf{t}^T{:}[(\nabla_0\mathbf{v})^T - \mathbf{W}] - \rho_0\mathbf{b}\cdot\mathbf{v}\right\} dv$$

$$+ [\text{Surface Integral}] \tag{55}$$

with the regularization:

$$F_{2\gamma}(\mathbf{v},\mathbf{W},\mathbf{t}) = F_2(\mathbf{v},\mathbf{W},\mathbf{t}) - \frac{1}{2\gamma}\int_{V_0} |\text{skew}\,\mathbf{t}|^2\, dv \tag{56}$$

for linear analysis of membrane elements. Since we have skew $\mathbf{t} = 0$ in the limit for infinitesimal deformation, it is applicable for linear problems and some modifications are required for nonlinear cases.

Several suggestions already exist on the regularization for nonlinear problems in the literature. Ibrahimbegovic (1993) proposed the following form:

$$F_{2\gamma}(\mathbf{u},\mathbf{R},\mathbf{r}^*) = F_2(\mathbf{u},\mathbf{R},\mathbf{r}^*) - \frac{1}{2\gamma}\int_{V_0} |\text{skew}\,\mathbf{r}^*|^2\, dv. \tag{57}$$

This form is applicable only for isotropic materials because $\mathbf{r}^*$ is in general unsymmetric for anisotropic materials.

Simo et al. (1992) proposed the principle:

$$\prod_{2}(\mathbf{u},\mathbf{R},\mathbf{T}) = \int_{V_0}\{W_0([\mathbf{I}+\nabla_0\mathbf{u}]\cdot[\mathbf{I}+\nabla_0\mathbf{u}]^T) + \mathbf{T}{:}\text{skew}[\mathbf{R}^T\cdot(\mathbf{I}+\nabla_0\mathbf{u})^T] - \rho_0\mathbf{b}\cdot\mathbf{u}\}\, dv$$

$$+ [\text{Surface Integral}] \tag{58}$$

with the regularization:

$$\prod_{2\gamma}(\mathbf{u},\mathbf{R},\mathbf{T}) = \prod_{2}(\mathbf{u},\mathbf{R},\mathbf{T}) - \frac{1}{2\gamma}\int_{V_0} |\mathbf{T}|^2\, dv \tag{59}$$

where $\mathbf{T}$, a skew-symmetric stress measure, works as a Lagrange multiplier to enforce the condition that $\mathbf{R}^T\cdot(\mathbf{I}+\nabla_0\mathbf{u})^T =$ symmetric. However, for constructing assumed stress elements, this is not suitable for our objective, since $\mathbf{T}$ vanishes at equilibrium.

Here, we propose the regularized form to use the derived principles for nonlinear problems:

$$F_{1\gamma} = F_1 + \frac{1}{2\gamma}\int_{V_0} |\text{skew}(\mathbf{U}\cdot\mathbf{r}^*)|^2\, dv \tag{60}$$

where F_1 is defined in Eq. (1). Remember that AMD requires skew$(\mathbf{U}\cdot\mathbf{r}^*) = 0$, it can be easily seen that the Euler Eqs. (5) ~ (10) also satisfies the stationary condition of the regularized $\delta F_{1\gamma} = 0$.

The rate form of $F_{1\gamma}$ is given as

$$\dot{F}_{1\gamma} = \dot{F}_1 + \frac{1}{2\gamma}\int_{V_N} |\text{skew}(\dot{\mathbf{r}}^* + \mathbf{D}\cdot\boldsymbol{\tau}^N)|^2\, dv. \tag{61}$$

The Euler equations derived from $\delta \dot{F}_{1\gamma}$ are:

- Constitutive Relation (CR)

$$\frac{\partial \dot{W}(\mathbf{D})}{\partial \mathbf{D}} - \text{symm}\,[\dot{\mathbf{r}}^{\star} + \gamma^{-1}\,\boldsymbol{\tau}^{N}\cdot\text{skew}\,(\dot{\mathbf{r}}^{\star} + \mathbf{D}\cdot\boldsymbol{\tau}^{N})] = 0. \tag{62}$$

- Compatibility Condition (CC)

$$(\nabla^{N}\mathbf{v})^{T} - \mathbf{D} - \mathbf{W} - \gamma^{-1}\,\text{skew}\,(\dot{\mathbf{r}}^{\star} + \mathbf{D}\cdot\boldsymbol{\tau}^{N}) = 0. \tag{63}$$

AMB (skew $(\dot{\mathbf{r}}^{\star} + [(\nabla^{N}\mathbf{v})^{T} - \mathbf{W}]\cdot\boldsymbol{\tau}^{N}) = 0$), LMB, TBC, DBC remain unchanged. Now, we find the requirement that the regularized Euler Eqs. (62), (63), AMB etc. result in the previous forms (36) ~ (41). To see this, it suffices to prove that skew $(\dot{\mathbf{r}}^{\star} + \mathbf{D}\cdot\boldsymbol{\tau}^{N}) = 0$.

Using AMB and compatibility,

$$\begin{aligned}
0 &= \text{skew}\,(\dot{\mathbf{r}}^{\star} + [(\nabla^{N}\mathbf{v})^{T} - \mathbf{W}]\cdot\boldsymbol{\tau}^{N}) \\
&= \text{skew}\,[\dot{\mathbf{r}}^{\star} + \{\mathbf{D} + \gamma^{-1}\,\text{skew}\,(\dot{\mathbf{r}}^{\star} + \mathbf{D}\cdot\boldsymbol{\tau}^{N})\}\cdot\boldsymbol{\tau}^{N}] \\
&= \text{skew}\,[\dot{\mathbf{r}}^{\star} + \mathbf{D}\cdot\boldsymbol{\tau}^{N} + \gamma^{-1}\{\text{skew}\,(\dot{\mathbf{r}}^{\star} + \mathbf{D}\cdot\boldsymbol{\tau}^{N})\}\cdot\boldsymbol{\tau}^{N}] \\
&= \text{skew}\,[\{\text{skew}\,(\dot{\mathbf{r}}^{\star} + \mathbf{D}\cdot\boldsymbol{\tau}^{N})\}\cdot(\mathbf{I} + \gamma^{-1}\,\boldsymbol{\tau}^{N})].
\end{aligned} \tag{64}$$

If $(\mathbf{I} + \gamma^{-1}\,\boldsymbol{\tau}^{N})$ is positive definite, the Eq. (63) holds only if skew $(\dot{\mathbf{r}}^{\star} + \mathbf{D}\cdot\boldsymbol{\tau}^{N}) = 0$. Therefore, it is safer to choose

$$\gamma > -\tau_{\min} \tag{65}$$

where $\tau_{\min}$ is the minimum eigenvalue of $\boldsymbol{\tau}^{N}$.

For implementation of the three field mixed variational principle, we replace $\mathbf{U}$ by $\mathbf{R}^{T}\cdot(\mathbf{I} + \nabla_{0}\mathbf{u})^{T}$:

$$F_{2\gamma} = F_{2} - \frac{1}{2\gamma}\int_{V_0} |\,\text{skew}\,(\mathbf{R}^{T}\cdot(\mathbf{I} + \nabla_{0}\mathbf{u})^{T}\cdot\mathbf{r}^{\star})|^{2}\,dv \tag{66}$$

Notice that the sign of the regularization term has changed, to make the regularized complementary energy W_c positive definite in terms of the skew symmetric part of the stress.

Likewise for the four-field mixed variational principle, one can obtain:

$$G_{1\gamma} = G_{1} + \frac{1}{2\gamma}\int_{V_0} |\,\text{skew}\,(\mathbf{U}'\cdot\mathbf{r}^{\star'})|^{2}\,dv$$

$$G_{2\gamma} = G_{2} - \frac{1}{2\gamma}\int_{V_0} |\,\text{skew}\,(\mathbf{R}^{T}\cdot(\mathbf{I} + \nabla_{0}\mathbf{u})^{T}\cdot\mathbf{r}^{\star'})|^{2}\,dv. \tag{67}$$

Note that the hydrostatic pressure does not affect AMB.

The rate forms of (66), (67) are shown below.

$$\dot{F}_{2\gamma} = \dot{F}_{2} - \frac{1}{2\gamma}\int_{V_N} |\,\text{skew}\,(\dot{\mathbf{r}}^{\star} - \mathbf{W}\cdot\boldsymbol{\tau}^{N} + (\nabla^{N}\mathbf{v})^{T}\cdot\boldsymbol{\tau}^{N})|^{2}\,dv \tag{68}$$

$$\dot{G}_{2\gamma} = \dot{G}_{2} - \frac{1}{2\gamma}\int_{V_N} |\,\text{skew}\,(\dot{\mathbf{r}}^{\star'} - \mathbf{W}\cdot\boldsymbol{\tau}^{N} + (\nabla^{N}\mathbf{v})^{T}\cdot\boldsymbol{\tau}^{N})|^{2}\,dv. \tag{69}$$

3
Finite element modeling and numerical schemes

So far, the general forms of variational principles are discussed from the view point of continuum mechanics. In this section, we focus on numerical schemes to implement the principles for nonlinear

problems. To begin with, we discuss the spatial discretization of the principles. This is no longer a trivial process and there are certain requirements to establish robust finite element formulations. It is known that the LBB (Ladyszhenskaya-Babuska-Brezzi) condition plays a crucial role to judge the existence and stability of the finite element solutions based on mixed variational principles.

We consider only two-dimensional plane stress or strain problems in this paper, even though the concepts are also applicable for three dimensional cases without intrinsic difficulties. The element concepts are based on the four noded membrane elements as developed for linear elasticity by Cazzani and Atluri (1993) which has displacements, unsymmetric stress, and a drilling degree of freedom as independent fields. In this research, we extend the numerical schemes to deal with geometric as well as material nonlinearities. The hydrostatic pressure is also introduced to the fields independently to count for the incompressibility of the material. The basic performances are checked by patch tests and some benchmark tests in the last part of the section.

3.1
Discretization of the field variables

We consider here the field discretization based on finite element concepts to construct two types of elements. The first one is the formulation without volume constraints, using the three field principle (49) and the second one is the formulation with volume constraints (incompressibility is one such case), using the four field principle (51) which includes the hydrostatic pressure. In either case, each field variable should be discretized independently. We allocate displacements as nodal variables and the rest (stress parameters, rotation, and hydrostatic pressure) as internal or element variables. Herein lies the reason for calling the present element formulation as the 'hybrid stress element formulation'. Displacements are continuous (C^0 continuity) across the element borders, while the other element variables are discontinuous in general. It is preferable to use small numbers of parameters to discretize the fields in order—(i) to save computer resources, and (ii) to avoid spurious modes which make the elements stiffer. In the well-established isoparametric elements, displacements are interpolated through the isoparametric mapping from the Cartesian coordinates (x_i) to the natural coordinates (ξ_i) of the elements. For the assumed stress hybrid elements, the other field variables are interpolated using the natural coordinates as well to construct the least order coordinate invariant elements (Pian and Wu 1988; Cazzani and Atluri 1993). Now, we discuss the discretization of the fields individually for a single element (denoted by the superscript 'm').

3.1.1
Discretization of displacement (u)

In order to describe the motion of the body, we use Cartesian coordinates with base vectors ($\mathbf{e}_1, \mathbf{e}_2, \mathbf{e}_3$) so that the material is isotropic at least along the $\mathbf{e}_3$-axis and the field variables are homogeneous in $\mathbf{e}_3$ as well. Among these types of two dimensional deformation, we discuss two special cases—plane strain ($u_{3,i} = u_{i,3} = 0$ where $u_{i,j} = \dfrac{\partial u_i}{\partial x_j}$, $i, j = 1 \sim 3$) and plane stress ($r^*_{3i} = r^*_{i3} = 0$) cases. We start the investigation with the four noded quadrilateral elements, the simplest elements of their kind. The displacements in the m-th element can be interpolated by the same shape function as in the standard displacement-type four noded isoparametric elements.

$$u_i = N_\alpha(\xi_1, \xi_2)\, q^m_{i,\alpha} \tag{70}$$

where $i = 1 \sim 2$, $\alpha = 1 \sim 4$, u_1 and u_2 are the displacements along ($\mathbf{e}_1, \mathbf{e}_2$), respectively. The displacement parameters $q_{i,1} \sim q_{i,4}$ coincide with the displacements of each node. The number of displacement parameters in 8 and the functions N_α are given by:

$$N_\alpha(\xi_1, \xi_2) = \frac{1}{4}(1 + c_{1,\alpha}\xi_1)(1 + c_{2,\alpha}\xi_2) \tag{71}$$

where $(c_{1,\alpha}, c_{2,\alpha}) = (-1, -1), (1, -1), (1, 1), (-1, 1)$, for $\alpha = 1, 2, 3, 4$. For later use, we introduce the matrix notation:

$$\{u\} = \begin{Bmatrix} u_1 \\ u_2 \end{Bmatrix} = [N(\xi_1, \xi_2)]\,\{q^m\}. \tag{72}$$

We adopt the common notation, [ ] for matrices, { } and ⌊ ⌋ for 'column' and 'row' vectors, respectively. The gradient of displacement is also given as:

$$\{\nabla_0 u\} = \begin{Bmatrix} u_{1,1} \\ u_{2,1} \\ u_{1,2} \\ u_{2,2} \end{Bmatrix} = [B(\xi_1, \xi_2)] \{q^m\}. \tag{73}$$

In UL rate form, velocity field v is interpolated as;

$$\{v\} = [N(\xi_1^N, \xi_2^N)] \{\dot{q}^m\}. \tag{74}$$

$$\{\nabla_N v\} = \begin{Bmatrix} v_{1,1} \\ v_{2,1} \\ v_{1,2} \\ v_{2,2} \end{Bmatrix} = [B(\xi_1^N, \xi_2^N)] \{\dot{q}^m\}. \tag{75}$$

where (ξ_1^N, ξ_2^N) are the natural coordinates of the element at C_N state.

As shown in (70), (71), this shape function has no 'incompatible' modes. It is still possible to introduce an additional discontinuous strain field to construct so called 'sub-h' elements (Belytschko et al. 1988) which facilitate capturing shear bands that are thinner than the mesh size. In this research, we adopt the ordinary shape functions (70), (71), so that a shear band, if captured by the element, has about the same order of thickness as the element size ('iso-h' elements).

The present elements do not display any shear-locking, which is often observed in ordinary displacement type elements. (The comparison between the present elements and displacement-type elements is shown in Sect. 3.5.)

Displacements along $\mathbf{e}_3$ direction need not be considered as long as the three field formulation (49) is adopted. Whereas, some modifications will be required to implemment the four field formulation (51) due to the existence of pressure field in the formulation. This point is discussed again in the forthcoming Sect. (3.2).

3.1.2
Discretization of rotation field (R)

Since all the kinematics are restricted to $(\mathbf{e}_1, \mathbf{e}_2)$ plane, we need to consider the rotation θ or the spin $W(=\dot{\theta})$ around $\mathbf{e}_3$ axis only. Reasonable choices, using one, three,... parameters respectively, are:

$$W(\xi_1, \xi_2) = \omega_0^m$$

$$W(\xi_1, \xi_2) = \omega_0^m + \omega_1^m \xi_1^N + \omega_2^m \xi_2^N$$

$$\vdots \tag{76}$$

We may increase the number of parameters to 4 or more. However, it is known that the incrase of the kinematic parameters may result in the increase of stress parameters to suppress the zero energy modes. Numerical studies (Cazzani and Atluri 1993) show that one parameter is enough to represent the rotation field if 6-stress parameters are taken. Therefore, we choose one parameter model $W(\xi_1, \xi_2) = \omega_0$ in which the parameter ω_0 can be associated with a rigid rotation of the centroid of the element. For later convenience, we introduce the matrix notation:

$$\{W\} = \begin{Bmatrix} W_{1,1} \\ W_{1,2} \\ W_{2,1} \\ W_{2,2} \end{Bmatrix} = \begin{Bmatrix} 0 \\ -\omega_0 \\ \omega_0 \\ 0 \end{Bmatrix} = [\Omega] \{\omega^m\} \tag{77}$$

where $[\Omega]$ is the shape function for the spin and $[\Omega] = [0 \ -1 \ 1 \ 0]^T$ in this one parameter model.

3.1.3
Discretization of hydrostatic pressure (p)

For incompressible materials, the hydrostatic pressure field p is required in the constitutive relations, and also, the pressure parameters are kept as unknowns in the global stiffness equation. The discretization of p is similar to the rotation field shown below:

$$\dot{p}(\xi_1, \xi_2) = \dot{p}_0^m$$

$$\dot{p}(\xi_1, \xi_2) = \dot{p}_0^m + \dot{p}_1^m \xi_1^N + \dot{p}_2^m \xi_2^N$$

$$\vdots \tag{78}$$

Since the increase of the parameters may cause locking of the elements, we also choose a one parameter model with $\dot{p} = \dot{p}_0$. Likewise, we introduce the matrix form:

$$\dot{p} = [P]\{\dot{p}^m\}. \tag{79}$$

The volume constraint holds in an average sense if one parameter discretization $[P] = [1]$ is used.

3.1.4
Discretization of stress ($\mathbf{r}^*$ or $\mathbf{r}^{*'}$)

So far, the discretizations of the kinematic fields ($\mathbf{u}, \mathbf{R}$) and the pressure p have been introduced. For discretizing the stress field, it should be considered that the following condition needs to be met to suppress all the kinematic modes.

$$s \geqq d - r \tag{80}$$

where s is the number of stress parameters; d is the number of kinematic parameters; and r is the number of the rigid body modes. The necessary (but not sufficient) condition (80) comes from the discrete LBB condition or the rank condition. See Ying and Atluri (1983), Xue et al. (1985). Strictly speaking, in order to guarantee the stability of the solution, we need to prove that the constant, which appears in the inequality of the LBB condition, is independent of the mesh size. This problem is extensively studied by Oden and his coworkers (Oden et al. 1982; Oden and Jacquotte 1984), but we do not go into the details here. It is also known that if stability and convergence are achieved, the least order stress parameters can be given by the equality in (80). Since we have $d = 9$ (displacement: 8 parameters; and rotation: 1 parameter) and $r = 3$, the preferable number for s is 6. In the earlier works of the assumed stress hybrid elements, stress components are interpolated using Cartesian coordinates of physical space.

In Murakawa's element (1978), stress functions, which are expressed as complete polynomials in Cartesian coordinates, are used. Therefore, at least 10 stress parameters are required for four noded plane elements to achieve coordinate invariance. Pian and Sumihara (1983) reduced stress parameters to 5 (using symmetric stress) for the same types of elements by utilizing the natural coordinates of the elements. Punch and Atluri (1984) constructed the least order [two versions of 5 parameter] assumed stress finite elements based on symmetry group theory. The least number is 6 in the formulation using unsymmetric stress as shown by Cazzani and Atluri (1993).

If the natural coordinates, instead of Cartesian coordinates, are used, the linear momentum balance holds only in an average sense. Hence, the elements have some distortion sensitivity which will be shown by benchmark tests in the forthcoming Sect. 3.5.

There are several ways to represent stress components by the natural coordinates and Cazzani and Atluri (1993) investigated the following five cases for linear problems. To avoid confusion, we use $i, j, \ldots$ to represent Cartesian components, $I, J, \ldots$ for covariant (by subscripts) or contravariant (by superscripts) components.

(i) Stress shape functions are expressed in the natural coordinates, but stress components are assumed to be Cartesian:

$$\dot{\mathbf{r}}^* = \dot{r}_{ij}^* \mathbf{e}_i \mathbf{e}_j$$

$$\{\dot{r}_{ij}^*\} = [\mathscr{A}]\{\dot{\beta}^m\} \tag{81}$$

where $\dot{r}^*_{ij}$; the Cartesian components, $[\mathscr{A}]$; shape function for stresses, and $\{\dot{\beta}^m\}$; stress parameters:

$$\{\dot{r}^*_{ij}\} = \begin{Bmatrix} \dot{r}^*_{11} \\ \dot{r}^*_{12} \\ \dot{r}^*_{21} \\ \dot{r}^*_{22} \end{Bmatrix}, \quad [\mathscr{A}] = \begin{bmatrix} 1 & & & \xi_2^N \\ & 1 & & \\ & & 1 & \\ & & & 1 \quad \xi_1^N \end{bmatrix}, \quad \{\dot{\beta}^m\} = \begin{Bmatrix} \dot{\beta}_1 \\ \dot{\beta}_2 \\ \dot{\beta}_3 \\ \dot{\beta}_4 \\ \dot{\beta}_5 \\ \dot{\beta}_6 \end{Bmatrix}. \tag{82}$$

(ii) Stress shape functions are expressed in the natural coordinates, and are assumed to be contravariant (curvilinear) convected components:

$$\dot{\mathbf{r}}^* = \dot{r}^{*IJ}\mathbf{g}_{IJ}$$

$$\{\dot{r}^{*IJ}\} = [\mathscr{A}]\{\dot{\beta}^m\} \tag{83}$$

where $\dot{r}^{*IJ}$ are the contravariant components, $(\mathbf{g}_I, \mathbf{g}_J)$ are covariant convected base vectors.

(iii) Stress shape functions are expressed in the natural coordinates, and are assumed to be covariant (curvilinear) convected components:

$$\dot{\mathbf{r}}^* = \dot{r}^*_{IJ}\mathbf{g}^I\mathbf{g}^J$$

$$\{\dot{r}^*_{IJ}\} = [\mathscr{A}]\{\dot{\beta}^m\} \tag{84}$$

where $\dot{r}^*_{IJ}$ are the covariant components $(\mathbf{g}^I, \mathbf{g}^J)$ are contravariant convected base vectors.

(iv) Stress shape functions are expressed in the natural coordinates, and are assumed to be contravariant components referred to the centroidal base vectors:

$$\dot{\mathbf{r}}^* = \dot{r}^{*IJ}\hat{\mathbf{g}}_I\hat{\mathbf{g}}_J$$

$$\{\dot{r}^{*IJ}\} = [\mathscr{A}]\{\dot{\beta}^m\} \tag{85}$$

where $\dot{r}^{*IJ}$ are the contravariant components, $(\hat{\mathbf{g}}_I, \hat{\mathbf{g}}_J)$ are covariant centroidal base vectors.

(v) Stress shape functions are expressed in the natural coordinates, and are assumed to be covariant components referred to the centroidal base vectors:

$$\dot{\mathbf{r}}^* = \dot{r}^*_{IJ}\hat{\mathbf{g}}^I\hat{\mathbf{g}}^J$$

$$\{\dot{r}^*_{IJ}\} = [\mathscr{A}]\{\dot{\beta}^m\} \tag{86}$$

where $\dot{r}^*_{IJ}$ are the covariant components, $(\hat{\mathbf{g}}^I, \hat{\mathbf{g}}^J)$ are contravariant centroidal base vectors.

According to Cazzani and Atluri (1993), choices (ii), (iii) do not pass the patch test. Among (i), (iv), (v), the element (iv) shows the best result (less sensitive to element distortion). Therefore, it is reasonable to adopt the element (iv) for nonlinear problems.

In element (iv), the Cartesian components $\dot{r}^*_{ij}$ are obtained from the contravariant components $\dot{r}^{*IJ}$ as follows:

$$\dot{r}^*_{ij} = (\hat{\mathbf{g}}_I \cdot \mathbf{e}_i)(\hat{\mathbf{g}}_J \cdot \mathbf{e}_j)\dot{r}^{*IJ} = J_{I\cdot i}J_{J\cdot j}\dot{r}^{*IJ} \tag{87}$$

where $J_{I\cdot i} = \hat{\mathbf{g}}_I \cdot \mathbf{e}_i$ is a Jacobean component of the element at the centroid.

Then, we have matrix representation:

$$\{\dot{r}^*_{ij}\} = [A]\{\dot{\beta}^m\} = [\mathscr{J}][\mathscr{A}]\{\dot{\beta}^m\} \tag{88}$$

where

$$[\mathscr{J}] = \begin{bmatrix} J_{1\,1}J_{1\,1} & J_{1\,1}J_{2\cdot 1} & J_{2\,1}J_{1\,1} & J_{2\cdot 1}J_{2\,1} \\ J_{1\,1}J_{1\cdot 2} & J_{1\,1}J_{2\cdot 2} & J_{2\,1}J_{1\cdot 2} & J_{2\cdot 1}J_{2\cdot 2} \\ J_{1\,2}J_{1\cdot 1} & J_{1\cdot 2}J_{2\cdot 1} & J_{2\,2}J_{1\cdot 1} & J_{2\,2}J_{2\cdot 1} \\ J_{1\cdot 2}J_{1\cdot 2} & J_{1\cdot 2}J_{2\,2} & J_{2\cdot 2}J_{1\,2} & J_{2\cdot 2}J_{2\,2} \end{bmatrix} \tag{89}$$

For later use, we introduce these representations as:

$$[A_{\text{symm}}] = [\mathscr{J}] \begin{bmatrix} 1 & & & & \xi_2^N & \\ & 1/2 & 1/2 & & & \\ & 1/2 & 1/2 & & & \\ & & & 1 & & \xi_1^N \end{bmatrix}$$

$$[A_{\text{skew}}] = [\mathscr{J}] \begin{bmatrix} 0 & & & & 0 & \\ & 1/2 & -1/2 & & & \\ & -1/2 & 1/2 & & & \\ & & & 0 & & 0 \end{bmatrix} \tag{90}$$

so that we have:

$$[A_{\text{symm}}]\{\dot{\beta}^m\} = \text{symmetric part of } \dot{r}^*_{ij}$$

$$[A_{\text{skew}}]\{\dot{\beta}^m\} = \text{skew part of } \dot{r}^*_{ij}. \tag{91}$$

To implement the four field formulation, $\dot{\mathbf{r}}^*$ can be discretized using the same shape function.

3.2
Reduction from general 3-D field formulation to 2-D formulation

Since the principles are derived from general three dimensional theory, the stress and strain components associated with $\mathbf{e}_3$ (r^*_{33} and $u_{3,3}$) are involved in the formulation even if a plane stress or strain condition is imposed. Therefore, some considerations on the reduction of the dimension of the space from 3-D to 2-D are required.

In the following, $(\,)_{ij}$ means the Cartesian components of a tensor and subscripts $i, j, k, l, \ldots$ run from 1 to 3, whereas $\alpha, \beta, \gamma, \delta, \ldots$, from 1 to 2.

In three field formulation (without p), the stress component r^*_{33} does not do any work for either the plane stress or strain case, so we can simply drop r^*_{33} and $u_{3,3}$ from the principle (since one of which vanishes). The plane stress or strain condition can be imposed through the following way. Suppose we have a rate form of the constitutive relation.

$$D_{ij} = [c]_{ijkl} \frac{1}{2}(\dot{r}^*_{kl} + \dot{r}^*_{lk})$$

$$\frac{1}{2}(\dot{r}^*_{ij} + \dot{r}^*_{ji}) = [e]_{ijkl} D_{kl} \tag{92}$$

where $[c]_{ijkl}$ and $[e]_{ijkl}$ are tangent compliance and elasticity matrices, respectively. For plane stress condition, we have $\dot{r}^*_{3i} = \dot{r}^*_{i3} = 0$, and the rate of complementary energy is given by:

$$\dot{W}_c(\text{symm}\,\dot{\mathbf{r}}^*) = \frac{1}{2} \cdot [c']_{\alpha\beta\gamma\delta} \cdot \frac{1}{2}(\dot{r}^*_{\alpha\beta} + \dot{r}^*_{\beta\alpha}) \cdot \frac{1}{2}(\dot{r}^*_{\gamma\delta} + \dot{r}^*_{\delta\gamma}) \tag{93}$$

where $[c']_{\alpha\beta\gamma\delta}$ is the submatrix of $[c]_{ijkl}$ obtained by deleting components associated with $\mathbf{e}_3$.

For plane strain condition, using $D_{3i} = D_{i3} = 0$,

$$\dot{W}_c(\text{symm}\,\dot{\mathbf{r}}^*) = \frac{1}{2} \cdot [e']^{-1}_{\alpha\beta\gamma\delta} \cdot \frac{1}{2}(\dot{r}^*_{\alpha\beta} + \dot{r}^*_{\beta\alpha}) \cdot \frac{1}{2}(\dot{r}^*_{\gamma\delta} + \dot{r}^*_{\delta\gamma}) \tag{94}$$

where $[e']_{\alpha\beta\gamma\delta}$ is the submatrix of $[e]_{ijkl}$ obtained by deleting components associated with $\mathbf{e}_3$.

In the four field formulation (with p), it is not as easy as in the three field formulation, since there is a coupling term in (49) as:

$$\frac{1}{3}\dot{r}^{*'}_{33}(v_{1,1} + v_{2,2} + v_{3,3}). \tag{95}$$

Since $\dot{r}^{*'}_{33} \neq 0$ even in plane stress case, we need an interpolation for $\dot{r}^{*'}_{33}$ as well as for $v_{3,3}$.

One option is, as taken by Reed and Atluri (1983), to discretize $\dot{r}^{*'}_{33}$, $v_{3,3}$ by adding some more parameters. (In this form, the plane stress/strain conditions are a posteriori satisfied.) The simplest form (one parameter each) is:

$$\begin{Bmatrix} \dot{r}^{*}_{11} \\ \dot{r}^{*}_{12} \\ \dot{r}^{*}_{21} \\ \dot{r}^{*}_{22} \\ \dot{r}^{*}_{33} \end{Bmatrix} = \begin{bmatrix} A & \\ & 1 \end{bmatrix} \begin{Bmatrix} \dot{\beta}_1 \\ \vdots \\ \dot{\beta}_6 \\ \dot{\beta}_7 \end{Bmatrix} = [\bar{A}]\{\dot{\beta}^m\}, \quad \begin{Bmatrix} v_{1,1} \\ v_{2,1} \\ v_{1,2} \\ v_{2,2} \\ v_{3,3} \end{Bmatrix} = \begin{bmatrix} B & \\ & 1 \end{bmatrix} \begin{Bmatrix} \dot{q}_1 \\ \vdots \\ \dot{q}_8 \\ \dot{q}_9 \end{Bmatrix}. \tag{96}$$

For later use, we introduce matrices $[B_v]$ and $[\bar{B}]$ such as:

$$v_{1,1} + v_{2,2} + v_{3,3} = [B_v]\{\dot{q}^m\}$$

$$\left\{ v_{i,j} + \frac{1}{3}\delta_{ij}(v_{1,1} + v_{2,2} + v_{3,3}) \right\} = [\bar{B}]\{\dot{q}^m\}. \tag{97}$$

As shown, the above can be developed in a straightforward manner and we develop the formulations based on this form. However, we can also construct element formulations without increasing the parameters by satisfying plane stress/strain conditions a priori to eliminate $\dot{r}^{*'}_{33}$ and $v_{3,3}$.

For the plane stress case, it can be enforced by using:

$$0 = \dot{t}_{33} = \dot{r}^{*'}_{33} - \frac{1}{3}(\dot{r}^{*'}_{11} + \dot{r}^{*'}_{22} + \dot{r}^{*'}_{33}) + \dot{p}$$

$$\frac{\partial \dot{W}_c}{\partial \dot{p}} = v_{1,1} + v_{2,2} + v_{3,3}. \tag{98}$$

For the plane strain case, we can use the constitutive relation:

$$\dot{r}^{*'}_{33} = [e]_{33ij} D'_{ij} \tag{99}$$

and the compatibility condition:

$$D'_{\alpha\beta} = v_{\alpha,\beta} - W_{\alpha\beta} - \frac{1}{3}(v_{1,1} + v_{2,2})$$

$$D'_{33} = -\frac{1}{3}(v_{1,1} + v_{2,2}). \tag{100}$$

Thus, $\dot{r}^{*}_{33}$, $v_{3,3}$ are given in terms of $\dot{r}^{*'}_{11}$, $\dot{r}^{*'}_{22}$, $v_{1,1}$, $v_{2,2}$, $W_{\alpha\beta}$ and $\dot{p}$.

For the plane strain case ($U_{31} = U_{32} = 0$, $U_{33} = 1$), there is another option at the risk of sacrificing some of the generality. One can perform the following multiplicative decomposition:

$$U'_{\alpha\beta} = U_{\alpha\beta} J^{-1/2} \quad \text{where } J = \det(U_{\alpha\beta}) \tag{101}$$

instead of the factor $J^{-1/3}$ used in (17). Since all the $\mathbf{e}_3$ components can be dropped, this may provide the simplest form for the plane strain problems with volume constraints.

3.3
Discretized variational principles

Now we are ready to discuss the discretized variational principles based on finite element concepts. Instead of seeking $(\mathbf{v}, \mathbf{W}, \dot{\mathbf{r}}^*)$ in the continuous field theory (49), we try to find $(\mathbf{v}^h, \mathbf{W}^h, \dot{\mathbf{r}}^{*h})$

$= \prod_m (\mathbf{v}^m, \mathbf{W}^m, \dot{\mathbf{r}}^{*m})$ as an approximate solution in finite dimensional space which satifies the stationary

condition of the discretized principle such that (49):

$$\dot{F}_2(\mathbf{v}^h, \mathbf{W}^h, \dot{\mathbf{r}}^{*h}) = \sum_m \Bigg(\int_{V_{N\,m}} \Big\{ -\dot{W}_c(\operatorname{symm} \dot{\mathbf{r}}^{*m}) - \frac{1}{2}\boldsymbol{\tau}^N : (\mathbf{W}^m \cdot \mathbf{W}^{mT}) + \boldsymbol{\tau}^{NT} : [\mathbf{W}^{mT} \cdot (\nabla_N \mathbf{v}^m)^T] + (\dot{\mathbf{r}}^{*m})^T : [(\nabla_N \mathbf{v}^m)^T - \mathbf{W}^m] - \rho_N \dot{\mathbf{b}} \cdot \mathbf{v}^m \Big\} dv - \int_{\partial V_{N,m} \cap S_{\sigma N}} \dot{\bar{\mathbf{T}}} \cdot \mathbf{v}^m \, ds - \int_{\partial V_{N,m} \cap S_{uN}} (\dot{\mathbf{t}}^{mT} \cdot \mathbf{n}) \cdot (\mathbf{v}^m - \bar{\mathbf{v}}) \, ds \Bigg) \tag{102}$$

where $\partial V_{N,m}$ is the boundary of the m-th element.

The stationary condition $\delta \dot{F}_2(\mathbf{v}^h, \mathbf{W}^h, \dot{\mathbf{r}}^{*h}) = 0$ gives the following:

$$\delta \dot{F}_2(\mathbf{v}^h, \mathbf{W}^h, \dot{\mathbf{r}}^{*h}) = \sum_m \Bigg(\int_{V_{N\,m}} \Big\{ \Big[-\frac{\partial \dot{W}_c(\operatorname{symm} \dot{\mathbf{r}}^{*m})}{\partial (\dot{\mathbf{r}}^{*m})^T} + (\nabla_N \mathbf{v}^m)^T - \mathbf{W}^m \Big] : \delta (\dot{\mathbf{r}}^{*m})^T + (\dot{\mathbf{r}}^{*m} + [(\nabla_N \mathbf{v}^m)^T - \mathbf{W}^m] \cdot \boldsymbol{\tau}^N) : \delta \mathbf{W}^m + [\nabla_N \cdot (\dot{\mathbf{r}}^{*m} - \boldsymbol{\tau}^N \cdot \mathbf{W}^m) + \rho_N \dot{\mathbf{b}}] \cdot \delta \mathbf{v}^m \Big\} dv + \int_{\partial V_{N\,m}} (\dot{\mathbf{t}}^{mT} \cdot \mathbf{n}) \cdot \mathbf{v}^m \, ds - \int_{\partial V_{N,m} \cap S_{\sigma N}} \dot{\bar{\mathbf{T}}} \cdot \delta \mathbf{v} \, ds - \int_{\partial V_{N,m} \cap S_{uN}} (\delta \dot{\mathbf{t}}^T \cdot \mathbf{n}) \cdot (\mathbf{v} - \bar{\mathbf{v}}) \, ds \Bigg). \tag{103}$$

Since the velocities are allocated as nodal variables, the velocity field is C^0 continuous and the compatibility across the elements is automatically satisfied. Suppose that the element m and n have a common edge $\rho_m \cap \rho_n$, and $\mathbf{n}$ is the outward normal vector to the edge of the element m, then $(-\mathbf{n})$ is the normal for the element n of the same edge. Hence, the surface integral in (103) becomes:

$$\sum_m \Bigg(\int_{\partial V_{N,m} \cap \partial V_{N\,n}} [(\dot{\mathbf{t}}^m - \dot{\mathbf{t}}^n)^T \cdot \mathbf{n}] \cdot \delta v^m \, ds + \int_{\partial V_{N,m} \cap S_{\sigma N}} ((\dot{\mathbf{t}}^m)^T \cdot \mathbf{n} - \dot{\bar{\mathbf{T}}}) \cdot \delta \mathbf{v}^m \, ds - \int_{\partial V_{N,m} \cap S_{uN}} (\delta (\dot{\mathbf{t}}^m)^T \cdot \mathbf{n}) \cdot (\mathbf{v}^m - \bar{\mathbf{v}}) \, ds \Bigg). \tag{104}$$

Therefore, the stationary condition of the finite element formulation provides the weak forms of

(i) constitutive relation, linear momentum balance, and angular momentum balance in each element.

(ii) traction and displacement boundary condition at each element boundary.

(iii) interelement traction reciprocity conditions.

The same results can be seen easily for the discretized four field formulation $\dot{G}_2(\mathbf{v}^h, \mathbf{W}^h, \dot{\mathbf{r}}^{*'h}, \dot{p}^h)$. The matrix forms of the discretized variational principles (inlcuding regularization terms) are given in Appendix-I.

3.4
Finite element assembly and strategy for numerical solution

Now, we move to the discussion on the finite element assembly and solution strategy of the system of equations, (mixed stiffness equation) derived from the discretized principles. Since the stress parameters are eliminated at each element, the resulting 'assumed stress' method has only kinematic field parameters (velocity and spin) in the three field formulation. On the other hand, in the four field formulation, the mixed stiffness equation involves hydrostatic pressure parameters additionally. The mixed stiffness equations are solved by the standard Newton-Raphson procedure with simple load/displacement incremental method or with the arclength method.

3.4.1
Elimination of stress parameters β

It is a common practice to eliminate β's from the mixed stiffness equations at each element level to reduce the number of unknowns in the mixed stiffness equation. As stated before, it is not possible without the regularization. (It can be easily checked that $[H^m_{\beta\beta}]$ is not invertible, where $[H^{m*}_{\beta\beta}]$ is invertible.

See Appendix-I.) In the earlier formulation of Murakawa and Atluri (1978), both the stress as well as the rotation parameters were eliminated simultaneously, without encountering any singular matrices. Singular matrices arise in this formulation, if only β's are to be eliminated, without using regularization.

As for the spin parameters ω, it is optional. If we retain ω's as global variables, it is possible to impose rotational boundary conditions at each element and this is advantageous for some shell problems. Therefore, we keep ω as unknowns in the mixed stiffness equation.

As for pressure parameter $\dot{p}$, it is not possible to eliminate it at element level if the material is perfectly incompressible because $[H_{pp}] = 0$. (If the material is compressible, it is possible. Another case when we can eliminate $\dot{p}$ for incompressible materials is in plane stress problems.) In the present formulation, we keep $\dot{p}$'s for generality.

The resulting single element stiffness equations for the three- and four-field formulations are given in Appendix-II.

The whole stiffness equation can be obtained by summing up the equations at each element and node.

3.4.2
Newton-Raphson method and Arclength method

The Newton-Raphson method is used for wide range of nonlinear problems and it is also applicable for the present element formulations. The method includes an iterative process to find an 'unknown' state C_{N+1} starting from the 'known equilibrated' state C_N. The details are given in Appendix-III. However, if there are an unstable phenomena such as limit load and bifurcation processes, it is difficult to prescribe the loading and displacement conditions as a single value function of time. In such a case, the problem can be solved by specifying the increment in the variables to a given amount, or so called 'arclength' δl. This scheme, introduced by Rikes (1972), is called the arclength method. Crisfield (1983) modified the method suitable for finite element analysis using the 'modified' Newton-Raphson method. However, the 'standard' Newton-Raphson method is also applicable and it is difficult to say which is more efficient in general. For more details, see Crisfield (1983) and Kondo and Atluri (1985).

3.5
Eigenvalues, patch tests and benchmark problems

So far, two types of element formulation are presented. The first one (three field formulation) has $(\mathbf{u}, \mathbf{R}, \mathbf{r}^*)$ as independent variables and is called the compressible element. The second, $(\mathbf{u}, \mathbf{R}, \mathbf{r}^*, p)$ as independent variables, and is called the incompressible element. It should be noted that the second type of elements can be applicable for nearly incompressible and even compressible materials if we use a finite bulk modulus. However, it is called so because the main objective is to develop the second type of elements for precise incompressibility problems.

Before moving on to the application, the basic performance of the both compressible and incompressible elements are checked by some benchmark tests and the results are summarized in the following. Since the above formulations are extensions of the elements by Cazzani and Atluri (1993) to highly nonlinear problems, the behavior of the elements for linear problems is equivalent to that of Cazzani's. Therefore, the main focus in the following is on nonlinear problems.

3.5.1
Eigenvalues

First, the eigenvalues of the stiffness matrix of a single perfectly square element are checked at its undeformed state. The eigenvalues are equal to those of Cazzani's for linear case as stated before. In addition to that, it is also confirmed that the eigenvalues are unaffected by:

(i) Finite rigid rotation

(ii) The value of the regularization coefficient γ.

The test (i) is done by fixing one node and rotating the element by the angles 45°, 90°, and 180°. Then, the rotation is fixed and the stiffness matrix at the rotated state is calculated. The results show that the eigenvalues are unaffected by finite rigid rotation and no spurious or kinematic modes are detected.

The purpose of the test (ii) is to check that the proposed regularization is valid for geometrically nonlinear problems. The range of γ used here is $10^{-3}\,G \sim 10^{3}\,G$ where G is the shear modulus. This test is done at the initial state and the states after finite rotations as in (i).

3.5.2
Patch tests

The elements can pass the single element patch test with a minimum number of constraints such as:

(i) A trapezoidal element with one side constrained (Fig. 1a) and subject to uniform tension applied to the opposite side (linear analysis).

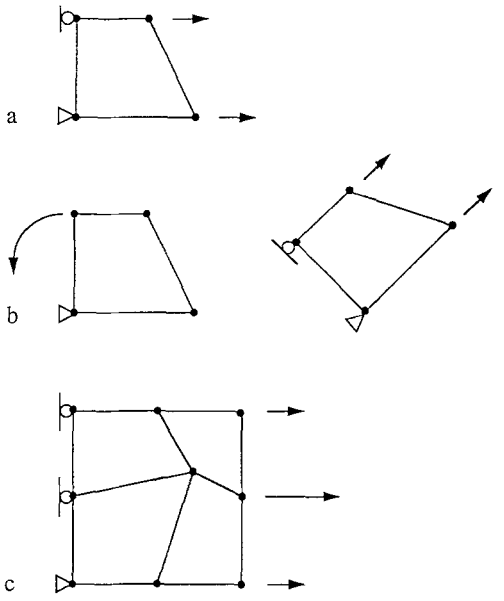

Fig. 1. Patch tests (a) Single skewed element with minimum constraints. (b) Finite rotation followed by stretching. (c) Assembly of elements

(ii) Fix the first node of the element in (i) and move the second node (by prescribed displacement condition) to rotate the element by angles 45°, 90°, and 180° respectively, and fix the second node and apply uniform tension to the opposite side (Fig. 1b).

(iii) The element configuration and the boundary condition is the same as (i) and (ii), but some nonlinear stress-strain relations such as Neo-Hookean and the power law type (introduced in the next section) are adopted and the element is stretched up to several hundred percent.

The test (i) is the same one as in Iura and Atluri (1992). The tests (ii) and (iii) are added in this reseach to check the element performance for geometrically and materially nonlinear problems. It can be seen that the elements also pass the multi-element patch test as shown in Fig. 1c once each element passes the above single element patch test.

3.5.3
Thin Cantilever beam

Some benchmark tests, e.g. the Cook's problem (Cook 1974), are also solved using the presented elements. As stated before, the results are the same as those in Cazzani and Atluri (1993) in linear case, so the details are omitted. Here, we demonstrate the thin cantilever beam undergoing finite rotation as a nonlinear benchmark problem since analytical solutions are known (as long as Hooke's law and the Euler-Bernoulli beam theory are valid). The tip deflection d vs. a tip load P is given as follows (Timoshenko and Goodier 1970):

$$\sqrt{\frac{PL^2}{EI}} = \int_{\phi}^{\pi/2} \frac{d\theta}{\sqrt{1-k^2\sin^2\theta}}, \quad \frac{d}{L} = 1 - 2\sqrt{\frac{EI}{PL^2}} \int_{\phi}^{\pi/2} \sqrt{1-k^2\sin^2\theta}\, d\theta \tag{105}$$

where

$$k = \sqrt{\frac{1+\sin\theta_{\text{end}}}{2}}, \quad \phi = \sin^{-1}\left(\frac{1}{\sqrt{1+\sin\theta_{\text{end}}}}\right) \tag{106}$$

L; length of the beam, E; Young's modulus, I; inertia of the cross section, and the rotation at the tip θ_{end} is used as a parameter. The problem is soved by the 'compressible' elements under plane stress condition with the regular and distorted meshes shown in Fig. 2a, b. The relation between the tip load and deflection (both are nondimensionalized) are shown in the Fig. 2d. Note that the nonlinearity in the response curve is due to geometrical nonlinearity, not from plasticity. For comparison, the solution by displacement-type four noded (Q4) and eight noded elements (Q8) are also shown in Fig. 2d. For Q4 and Q8, only regular meshes are used (shown in Fig. 2a and 2c). If the regular mesh is used, the result by the present hybrid elements coincides with the analytical result quite well as compared to the displacement-type elements. However, if the distorted mesh is used, the numerical solution deviates from the analytical solution as shown in the figure.

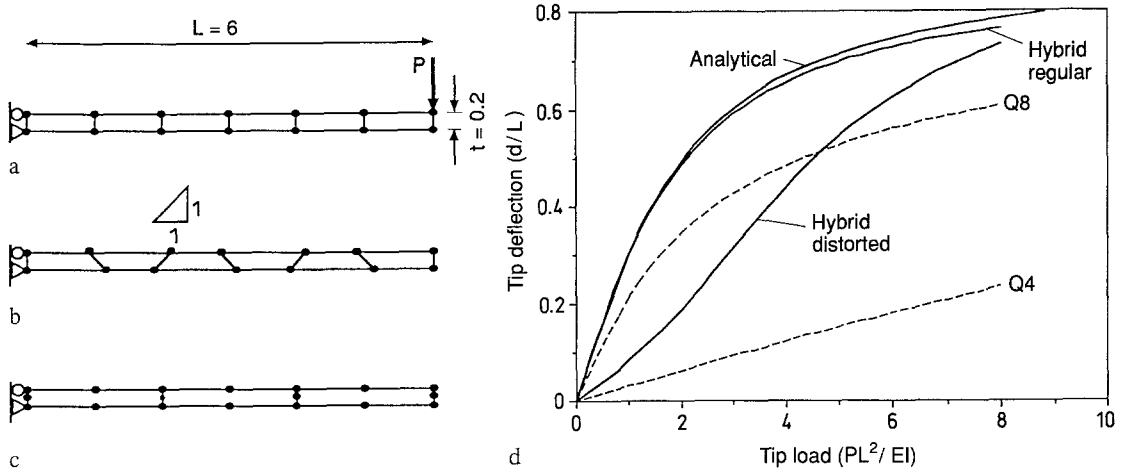

Fig. 2. Thin Cantilever beam. (a) Regular hybrid or Q4 elements (6-elements, 14-nodes). (b) Distorted elements. (c) Q8 elements (3-elements, 18-nodes). (d) Tip load-tip deflection curves of the beam

Once again, regardless of the element distortion, the element passes the linear and nonlinear patch tests if the deformation modes are simple stretching, shear, finite rigid body motion, and their combinations. But, element distortion makes the element stiffer in bending. The distortion sensitivity problem may stimulate further investigation on the element formulation.

4
Numerical examples of the shear localization problem

In this section, we present some numerical examples of shear localization problems solved by the assumed stress hybrid elements. The sample problems, given below, are selected to check the applicability of the presented element formulation for strain localization problems.

(i) Compression of a block.

(ii) Twisting of a tube.

In the following, only plane strain problems are treated and the materials are assumed to be perfectly incompressible, isotropic, and hyperelastic. The constitutive relations are derived from the strain energy functions with small number (3) of material constants.

First, we review briefly the criteria of shear localization and its relation with the constitutive relations. Numerical examples are presented and discussed.

4.1
Ellipticity of the material constitutive relation

The equilibrium condition of the finitely deformed body, in absence of body forces, is written in terms of the Cartesian components of the first Piola-Kirchhoff stress t_{ij}:

$$t_{ij,i} = 0. \tag{107}$$

We rewrite the equilibrium equation for displacements using the strain energy $W(\nabla_0 \mathbf{u})$:

$$t_{ij,i} = \frac{\partial}{\partial x_i}(t_{ij}) = \frac{\partial}{\partial x_i}\left(\frac{\partial W(\nabla_0 \mathbf{u})}{\partial u_{i,j}}\right) = \frac{\partial^2 W(\nabla_0 \mathbf{u})}{\partial u_{i,j}\partial u_{k,l}} u_{k,li} = e_{ijkl} u_{k,li} = 0. \tag{108}$$

The characteristic of the differential Eq. (108) depends on the elasticity coefficient e_{ijkl} and it is called strongly elliptic if the inequality:

$$e_{ijkl} m_i m_k n_j n_l > 0 \tag{109}$$

holds for every pair unit vectors **m**, **n**. (If the left hand side of (109) is negative for some **m** and **n**, it is called hyperbolic.) It is known that the Eq. (108) has a unique and smooth solution for a given boundary conditions if the inequality (109) holds. On the contrary, if the ellipticity fails, there may not exist a classical smooth solution. As a consequence, some characteristic lines (surfaces) may emerge on which the deformation gradient is discontinuous in the body. We call such a line (surface) as a shockline (shocksurface), which is also referred to as an equilibrium shock or an elastostatic shock in the literature.

'Shear band' means the area (usually very thin) surrounded by shocklines (shocksurfaces), within which the shear strain level is significantly higher than that on the outside. This phenomenon is also called shear localization.

Among the various cases, shear band formation in the incompressible material is of theoretical and practical interest. Any plane strain deformation of an incompressible body can be regarded locally as a simple shear followed by a rigid body rotation. Hence, the material consitutive relation can be completely specified by its stress-strain relation in simple shear. In the following, we denote $\tau(k)$ for stess in simple shear as a function of k; the amount of shear strain in simple shear. (Note that k is not equivalent to the shear component of stretch tensor.) We also assume that τ is an odd function of k, i.e. $\tau(-k) = -\tau(k)$. Therefore, we presume that $k \geqq 0$ in the following discussion. According to Abeyaratne and Knowles (1989), shockline(s) may exist in incompressible material under plane strain deformation if the inequality:

$$[\tau(k_1) - \tau(k_2)]\,[k_1 - k_2] \leqq 0 \tag{110}$$

holds for some $k_1 \neq k_2$. The Eq. (110) means that the slope of the stress-strain curve in simple shear becomes negative in some strain range.

Now, we introduce the constitutive relations which satisfy such a requirement through strain energy functions. It is a common practice to introduce strain energy function in terms of the invariants I_1, I_2 of the right (Cauchy-Green) deformation tensor $\mathbf{C} = (\mathbf{I} + \nabla_0 \mathbf{u})\cdot(\mathbf{I} + \nabla_0 \mathbf{u})^T$ for isotropic incompressible material, where $I_1 =$ trace $(\mathbf{C})$, $I_2 = \frac{1}{2}(I_1^2 - \mathbf{C}:\mathbf{C})$. Note that in the plane strain case, we have $I_1 = I_2$. The amount of shear strain, or simply shear strain k is calculated from $\mathbf{C}$ as:

$$k^2 = \text{trace}(\mathbf{C}) - 3 = I_1 - 3. \tag{111}$$

So k is another invariant of the deformation field and can be used instead of I_1, I_2. Note that in (111), we can replace $\mathbf{C}$ by the left (Cauchy-Green) deformation tensor $\mathbf{G}$.

In this research, the following hypothetical models are used:

Type I—Power Law

$$W(I_1) = \begin{cases} C_1(I_1 - 3) & \text{if } k \leqq k_0 \\ C_2(I_1 - 3)^n & \text{if } k > k_0 \end{cases}. \tag{112}$$

Type II—Strain Softening/Hardening

$$W(I_1) = \frac{C_1(I_1 - 3)}{1 + C_2(I_1 - 3)} + C_3(I_1 - 3)^2 \tag{113}$$

where C_1, C_2, C_3, n, k_0 are the material constants. In type I, we must have $C_2 = C_1 k_0^{(2-2n)}/n$ so that the shear stress-strain curve is continuous at $k = k_0$ (The differential of the curve is not continuous at this point). So the independent material constants are C_1, n, k_0 in this model and k_0 determines the 'critical' shear strain. This consitutive law is used in Abeyaratne and Yang (1987) for mode I crack problems. The form of the type II is chosen so that the material shows hardening in larger strain region. In this research, we use $C_1 = 1$, $n = 0.25$, $k_0 = 0.1$ for the type I and $C_1 = 1$, $C_2 = 10$, $C_3 = 0.05$ for the type II. C_1 (Types I, II) and C_3 (Type II) have the dimension of stresses and n, k_0 (Type I) and C_2 (Type II) are dimensionless quantities.

The stress-strain curves in simple shear are calculated by:

$$\tau = \frac{\partial W}{\partial k} = \frac{\partial W}{\partial I_1}\frac{\partial I_1}{\partial k} = 2k\frac{\partial W}{\partial I_1} \tag{114}$$

and the results for both models are shown in Fig. 3.

In the following analyses, no other material parameters are involved (such as threshold stress or shear band thickness, etc.) The shear band formation is triggered only from the characteristics of the given constitutive relations.

4.2
Example 1: Compression of a block

The first example is the compression of a block by uniaxial loads as shown in Fig. 4. A rectangular block with unit thickness is modeled by 16×32 perfectly square elements. (The size of a single element is

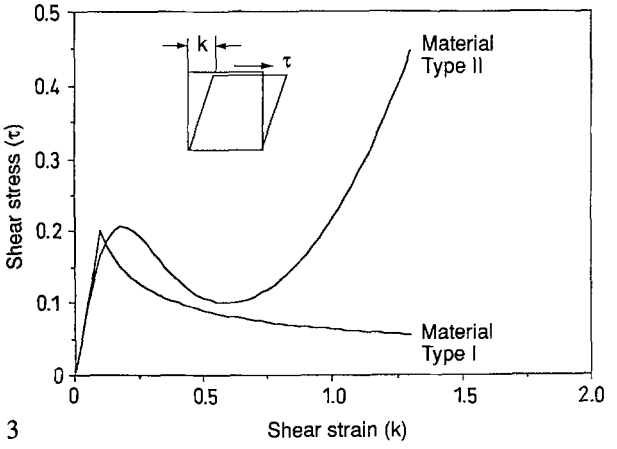

3

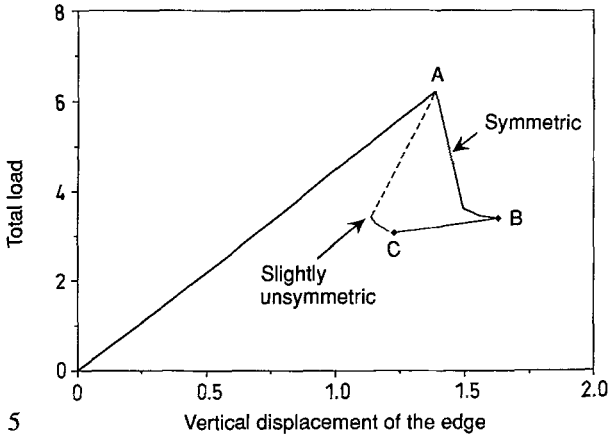

5

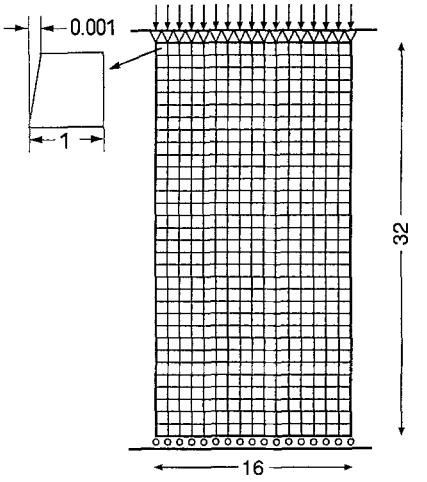

4

Figs. 3–5. 3 Stress-strain relation in simple shear for material type I and II. 4 Initial configuration and boundary conditions of the block compression problem (symmetric and slightly unsymmetric configuration). 5 The response (load-displacement curve) of the block compression problem from the finite element analysis

1×1.) The bottom edge is roller supported, the lateral sides are free, and the upper edge is fixed horizontally and pushed down in vertical direction. (Constrained displacement boundary conditions are imposed through the arclength method.) The material property (Type I—power law) is homogeneous throughout the block.

To check the sensitivity of the solution to the initial configuration, we also analyzed the second model whose symmetry in the initial configuration is slightly disturbed by moving the upper left corner node to the right by 0.001 as shown in Fig. 4.

Now, since the upper edge is fixed, it is expected that the stress concentration occurs at the upper left and right corners with the shear bands emerging from these corners. (Since the lower edge is roller supported, it does not occur at the bottom.) The global response curves (vertical displacement of the upper edge *vs.* total reactions from the edge) obtained by the finite element analysis are shown in Fig. 5. Up to the critical point (denoted by 'A' in the figure. 4.3% compression from the initial heights.), both perfectly symmetric and slightly unsymmetric models take almost the same paths. Moreover, no shocklines nor shear bands are observed. At point A, the shear band formulation starts at the upper corners as shown in the deformed mesh and the contour plot of shear strain k in Fig. 6. (In this paper, meshes and displacements are drawn to the same scale, so that the figures show the actual deformation. In the contour plots, the value k is calculated from displacements. In this formulation, it is also possible to calculate the strain field from the stress fields using the constitutive relations.) Note that in the area where the shear strain is greater than $k_0 = 0.1$, the material property becomes hyperbolic.

After passing point A, the two models take different paths. For the symmetric model, the load (reaction force) drops sharply and reaches point 'B', where the X shaped shear bands are developed as shown in Fig. 7. However, our numerical analysis shows that the symmetric deformation mode is unstable and another bifurcation occurs at point 'B'. One of the bands disappears and the deformation mode becomes unsymmetric at point 'C' as shown in Fig. 8. If the initial configuration is slightly unsymmetric, even though the imprefection is very small as assumed in the second model, we cannot find a symmetric deformation mode after the first critical point 'A' and the deformation mode goes immediately from symmetric 'A' to unsymmetric 'C'. From these observations, one may conclude that—(i) The shear band(s) tends to shrink as the deformation proceeds to stabilize itself. (ii) The deformation mode is

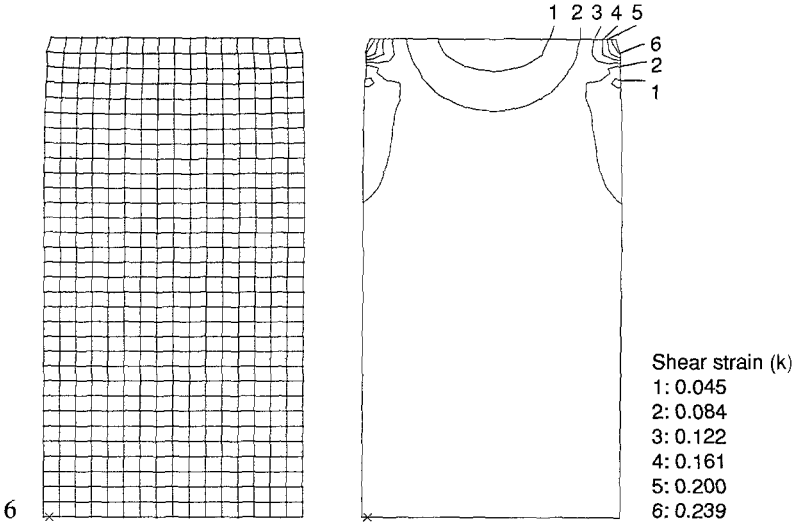

6

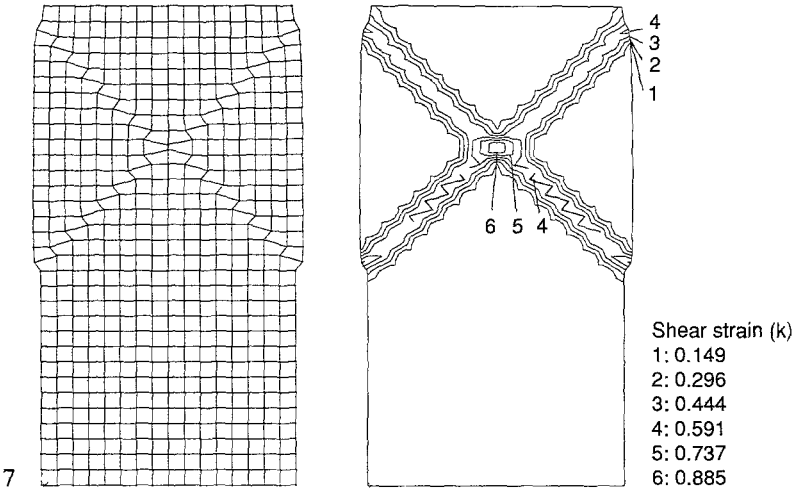

7

Figs. 6, 7. 6 Deformed mesh and shear strain distribution of the block at state 'A'. 7 Deformed mesh and shear strain distribution of the block at state 'B'

quite sensitive to the initial configuration. (There are some similarities with the buckling of a column by compressive axial loads.)

As stated before, once the ellipticity fails, the uniqueness of the solution is not guaranteed as shown in the finite element analysis. In this case, not only the deformed configuration but also the response curve (displacement-total load) cannot be determined uniquely. To see this, the following semi-inverse analysis is carried out by making simple kinematic assumptions as follows. As shown in Fig. 9, the block is decomposed into the two parts (I, II) and, in each area, the deformation gradient is homogeneous. There are two parallel shocklines which divides the area II, the shear band area, from the rest of the block (the area I). The area I is uniformly compressed in $\mathbf{e}_2$ direction with stretch ratio $\lambda(<1)$. Then, the deformation gradient $\mathbf{F}_I$ in the area I has the following matrix representation:

$$\mathbf{F}_I \sim \begin{bmatrix} (F_I)_{11} & (F_I)_{12} \\ (F_I)_{21} & (F_I)_{22} \end{bmatrix} = \begin{bmatrix} \lambda^{-1} & 0 \\ 0 & \lambda \end{bmatrix} \tag{115}$$

where $(F_I)_{ij}$ are the Cartesian (i,j) components with respect to the base vectors $\mathbf{e}_1$, $\mathbf{e}_2$ and the $\mathbf{e}_3$ components are omitted. $(F_I)_{11} = \lambda^{-1}$ comes from the incompressibility of the material.

Now, the continuity of displacements along the shockline requires the following (Abeyaratne and Knowles 1989):

$$\mathbf{F}_{II} = (\mathbf{I} + \kappa \mathbf{e}_1^* \mathbf{e}_2^*) \cdot \mathbf{F}_I \tag{116}$$

where $\mathbf{e}_1^*$, $\mathbf{e}_2^*$ are tangent and normal unit vectors of the shockline. The interpretation of (116) is that $\mathbf{F}_{II}$ can be regarded as a deformation $\mathbf{F}_I$ followed by a simple shear with amount κ. The transformation

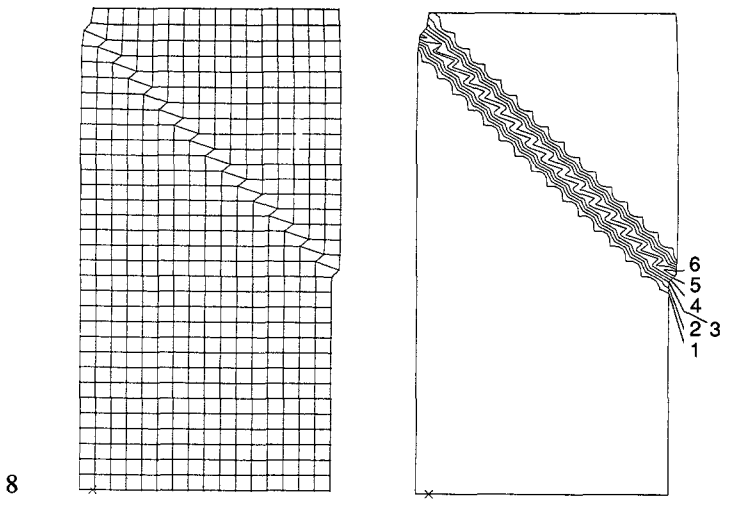

8

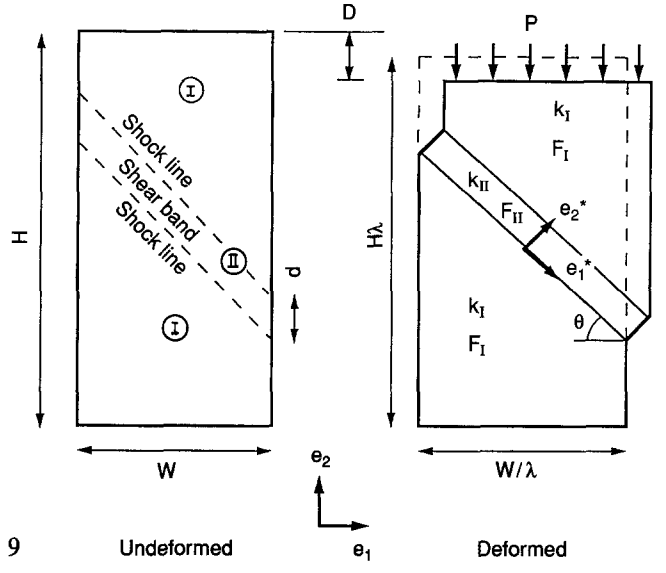

9

Figs. 8, 9. 8 Deformed mesh and shear strain distribution of the block at state 'C'. 9 A sketch of semi-inverse method for the block compression problem

rule of the tensor components shows that $\mathbf{F}_{II}$ has the matrix representation:

$$\mathbf{F}_{II} \sim \begin{bmatrix} c & -s \\ s & c \end{bmatrix}\begin{bmatrix} 1 & \kappa \\ 0 & 1 \end{bmatrix}\begin{bmatrix} c & s \\ -s & c \end{bmatrix}\begin{bmatrix} \lambda^{-1} & 0 \\ 0 & \lambda \end{bmatrix}$$

$$= \begin{bmatrix} \lambda^{-1}(1+cs\kappa) & \lambda^{-1}s^2\kappa \\ \lambda c^2\kappa & \lambda(1-cs\kappa) \end{bmatrix} \tag{117}$$

where $c = \cos\theta$ and $s = \sin\theta$. Now the equilibrium condition along the shocklone is met if (Abeyaratne and Knowles 1989):

$$\mathbf{e}_1^* \cdot \left[\left(\frac{\tau(k_I)}{k_I}\mathbf{G}_I - \frac{\tau(k_{II})}{k_{II}}\mathbf{G}_{II} \right) \cdot \mathbf{e}_2^* \right] = 0 \tag{118}$$

where $\mathbf{G}_I = \mathbf{F}_I \cdot \mathbf{F}_I^T$, $\mathbf{G}_{II} = \mathbf{F}_{II} \cdot \mathbf{F}_{II}^T$ are the left deformation tensors in the area I, II, respectively. By simple matrix algebra, we have:

$$\mathbf{G}_I \sim \begin{bmatrix} \lambda^{-2} & 0 \\ 0 & \lambda^2 \end{bmatrix}$$

$$\mathbf{G}_{II} \sim \begin{bmatrix} \lambda^{-2}(1+cs\kappa)^2 + \lambda^2 c^4\kappa^2 & \lambda^{-2}s^2\kappa(1+cs\kappa) - \lambda^2 c^2\kappa(1-cs\kappa) \\ \lambda^{-2}s^2\kappa(1+cs\kappa) - \lambda^2 c^2\kappa(1-cs\kappa) & \lambda^{-2}(1-cs\kappa)^2 + \lambda^{-2}s^4\kappa^2 \end{bmatrix}. \tag{119}$$

From the type I constitutive equation:

$$\frac{\tau(k_I)}{k_I} = 2C_1$$

$$\frac{\tau(k_{II})}{k_{II}} = 2C_1\left(\frac{k_{II}}{k_0}\right)^{2n-2} \tag{120}$$

where k_I and k_{II}, the amounts of the shear strain in areas I and II respectively, are obtained, remembering that a two dimensional expression is used, as follows:

$$k_I^2 = \text{trace}(\mathbf{G}_I) - 2$$

$$k_{II}^2 = \text{trace}(\mathbf{G}_{II}) - 2. \tag{121}$$

The above conditions (equilibrium and continuity of the displacements along the shockline) are not enough to determine all the unknowns (k_I, k_{II}, κ, and θ). Usually, we need another condition such as energy dissipativity to determine the shockline inclination θ. However, to simplify the problems, we make the kinematic assumptions such that $\theta = 45°$ and remains unchanged during the deformation. (This assumption is not exactly true in the finite strain case, but the following results are not very sensitive to θ if θ does not change largely during the deformation or if the shear band thickness is small.) Thus, solving (115) ~ (121), we can find κ, and the relation between the total load P and the displacement of the upper edge D is obtained from:

$$P = 2C_1 W(\lambda^{-3} - \lambda)$$

$$D = H(1-\lambda) + \kappa\lambda d/2 \tag{122}$$

where H, W are the heights and width of the block in the undeformed configuration. Now, d, the thickness of the shear band in the undeformed configuation, is another indeterminable quantity from equilibrium conditions. Here, we treat d as a parameter to calculate the relations of P and D and the results are shown in Fig. 10. For comparison, the result of the slightly unsymmetric model obtained by finite element analysis is overlapped in the figure by the dashed line. (The stress concentration at the upper corners makes the critical load by finite element analysis slightly lower.)

If we take the energy dissipativity into the consideration and presume that the block is an ideal continuum body, we can see $d \to 0$ in this way. Suppose that we compress the block until the edge displacement becomes, say, $D = 2$. In Fig. 10, the area below the each response curve represents the energy required to achieve such a compression. (e.g. the shaded area in Fig. 10 is the energy for $d = 0.5$.) Then, as shown, the smaller the shear band thickness d is, the smaller is the energy required for the compression. And in the limit as $d \to 0$, the energy also becomes zero. From the physical point of view, a material of this kind has a 'thickness' d as a intrinsic material constant which comes from the microscopic

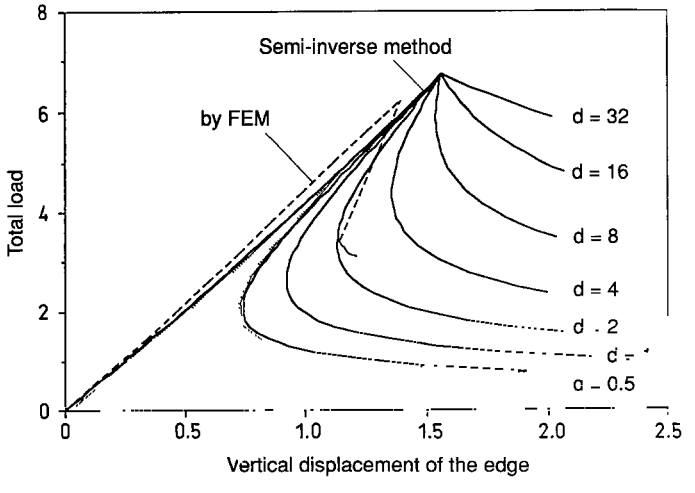

Fig. 10. The response (load-displacement) curves of the block compression problem comparison of FEM and the semi-inverse method (shear band thickness as a parameter)

structure of itself. In most of the finite element analyses, the mesh size plays a role of such a material constant unless it is a priori specified and involved in the formulation from the beginning, but the further discussions on this matter are beyond the scope of this paper.

As shown in Fig. 10 (and also from the observation of the deformed meshes), the elements capture the shear band with thickness $d = 2$ (width of two elements). This may be the smallest width that can be captured by the elements of this type, which do not involve an embedded shear localization field within each element.

Another important observation is that there are backlashes in loads as well as displacements after the critical point 'A', unless the shear band is unreasonably thick. Therefore, simple load or displacement control method breaks down after the critical point and the use of the arclength method is inevitable.

4.3
Example 2: Twisting of a tube

Abeyaratne (1981), Abeyaratne and Knowles (1987) extensively studied this problem since it provides good insights for the equilibrium shock problems, while it is simple enough to allow an analytical approach to some extent.

As different from the previous example, we consider the stability of the tube from the beginning. As a consequence, we do not observe shear bands and the material remains elliptic everywhere in the tube— even though a shockline exists. For the material (type I), as used in the block compression problem, the tube is not mechanically stable when the load exceeds the critical point. (Remember that, in the previous problem, the advent of the shear bands does not necessarily mean that the block becomes mechanically unstable.) Therefore, we use the type II material model—strain softening/hardening model—as the constitutive relation. We observe that a shockline is formed between the areas whose material properties are elliptic/elliptic in this example, whereas in the previous example, a shock occurs between elliptic/hyperbolic.

The geometry and the boundary conditions used in the finite element analysis are shown in Fig. 11. A tube with inner and outer radii $r_0 = 1$ and $r_1 = 1.8$ respectively, is modeled by 16×32 elements. The outer surface is fixed and the inner surface is twisted by uniformly distributed forces as shown. (The load is specified by the torque T.)

Before presenting the finite element analysis, we briefly review the analytical approach by Abeyaratne (1981). From the symmetry of the problem, we can expect that a point (r, θ) moves to $(r, \theta + \phi(r))$ by deformation and also that the normal components of stresses are irrelevant to the deformation. Hence, we need to consider only (Cauchy) shear stress component $\tau_{r\theta}(r)$, which can be given from the equilibrium condition as:

$$\tau_{r\theta}(r) = \frac{T}{2\pi r^2}. \tag{123}$$

Therefore, the problem is basically one dimensional and is solved by finding $\phi(r)$.

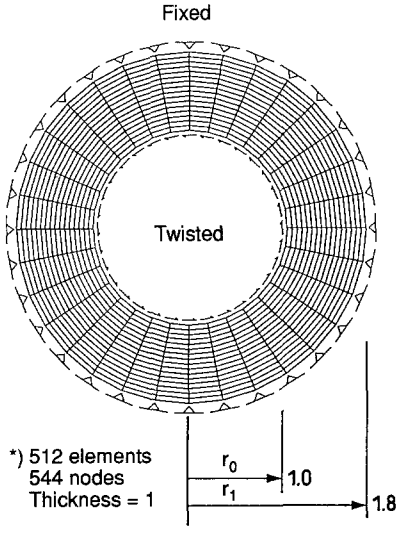

Fig. 11. Initial configuration and boundary conditions of the tube problem

There are three cases when the uniqueness of the solution is considered.

(i)	$0 \leqq T < 2\pi(r_0)^2 \tau_{\min}$	unique smooth solution, no shocks
(ii)	$2\pi(r_0)^2 \tau_{\min} \leqq T < 2\pi(r_1)^2 \tau_{\max}$	solution is not unique, there may/may not be shocks
(iii)	$2\pi(r_1)^2 \tau_{\max} \leqq T$	unique smooth solution, no shocks

In the following, we exclude the states invovling two or more shocks or the states wherein the local material property becomes hyperbolic, since those states are unstable. Now, the goal is to find the global mechanical response of the tube represented by the relation between the torque T and the twist $\phi_0 = \phi(r_0)$ at the inner surface. Since $\phi(r_1) = 0$, we have ϕ_0 as:

$$\phi_0 = \int_{r_1}^{r_0} \frac{\partial \phi(r)}{\partial r}\, dr \tag{124}$$

and the form $\phi(r)$ is determined through the shear strain $k(r)$ in the tube given by:

$$r \frac{\partial}{\partial r} \phi(r) = k(r) = f(\tau) \tag{125}$$

where $f(\tau) = k$ is the inverse map of $\tau = \tau(k)$. Since $f(\tau)$ is not a single valued function, we need the following three branches f_1, f_2, f_3 such that:

$$0 \leqq f_1(\tau) < k_1, \quad k_1 \leqq f_2(\tau) < k_2, \quad k_2 \leqq f_3(\tau) < \infty \tag{126}$$

where k_1, k_2 are shear strains corresponding to the maximum, minimum shear stresses, respectively (see Fig. 12b).

Then, from (123) ~ (126) we have:

$$\text{(i)} \quad \phi_0 = \int_{r_1}^{r_0} \frac{1}{r} f_1\left(\frac{T}{2\pi r^2}\right) dr$$

$$\text{(ii-a)} \quad \phi_0 = \int_{r_1}^{r_0} \frac{1}{r} f_1\left(\frac{T}{2\pi r^2}\right) dr$$

$$\text{(ii-b)} \quad \phi_0 = \int_{r_1}^{\bar{r}} \frac{1}{r} f_1\left(\frac{T}{2\pi r^2}\right) dr + \int_{\bar{r}}^{r_0} \frac{1}{r} f_3\left(\frac{T}{2\pi r^2}\right) dr$$

$$\text{(ii-c)} \quad \phi_0 = \int_{r_1}^{r_0} \frac{1}{r} f_3\left(\frac{T}{2\pi r^2}\right) dr$$

$$\text{(iii)} \quad \phi_0 = \int_{r_1}^{r_0} \frac{1}{r} f_3\left(\frac{T}{2\pi r^2}\right) dr. \tag{127}$$

The case (ii-b) includes shockline with the radius $\bar{r}$, and the response relation (Twist ϕ_0, Torque T) is not unique since $\bar{r}$ is arbitrary. To determine the deformation, we need to specify $\bar{r}$, or equivalently, the shear stress $\bar{\tau}$ on the shockline. As shown in Fig. 12a, b, if a shockline exists, there is a jump in the shear strain across the shock. At the point just inside the shock (P_-), the shear strain is in the region $[k_2, \infty]$, and just outside (P_+), k is in the region $[0, k_1]$. Actually, the shock can occur at any stress level between $\tau_{\min}$ and $\tau_{\max}$. The jump such that $[0, k_1] \leftrightarrow [k_1, k_2]$ or $[k_1, k_2] \leftrightarrow [k_2, \infty]$ is excluded since they are unstable. Abeyaratne proved that if the shock occurs with the characteristic stress τ_c, which is the stress level such that the shaded areas I, II in Fig. 12b are equal, the potential energy becomes a minimum. (This path $e \leftrightarrow f$ is called the Maxwell path.) However, this does not necessarily mean other states are unstable. If the torque T increases quasistatically from zero, the shock occurs at the stress $\tau_{\max}$ ($d \to b$ in Fig. 12b). And if we once make the torque T higher than $2\pi(r_1)^2 \tau_{\max}$ and reduce it quasistatically, the shock occurs at the stress $\tau_{\min}$ ($h \to g$ in Fig. 12b). If we switch loading/unloading while a shockline exists, we will have a state with a shock on which the stress is between $\tau_{\max}$ and $\tau_{\min}$.

Now, we present the results of the finite element analysis. In this example, the simple load incremental method is used to find stable configurations. The global response (Twist ϕ_0, Torque T) curve by finite element analysis (FEM) is shown in Fig. 13 overlapped with the analytical solution (dashed lines).

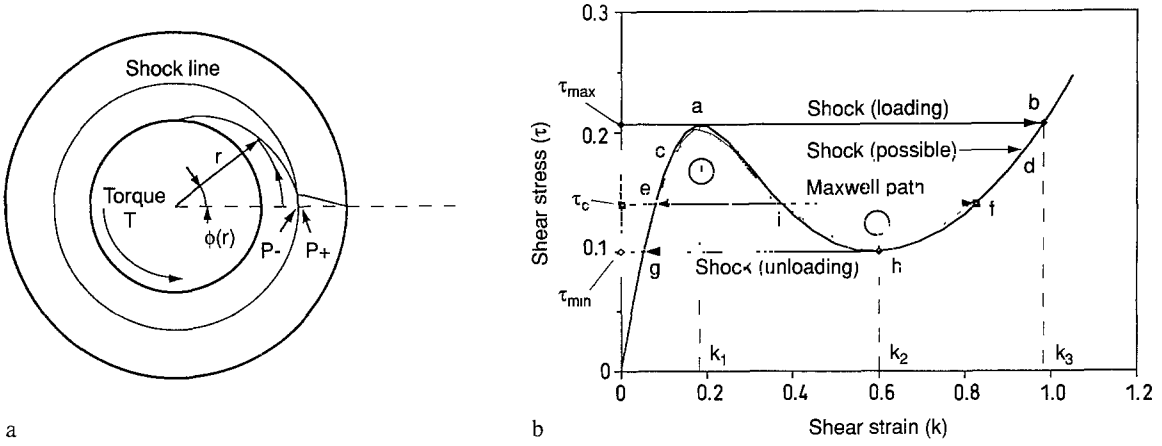

a b

Fig. 12. (a) A sketch of the shock in the tube. (b) Stress-strain relation in simple-shear

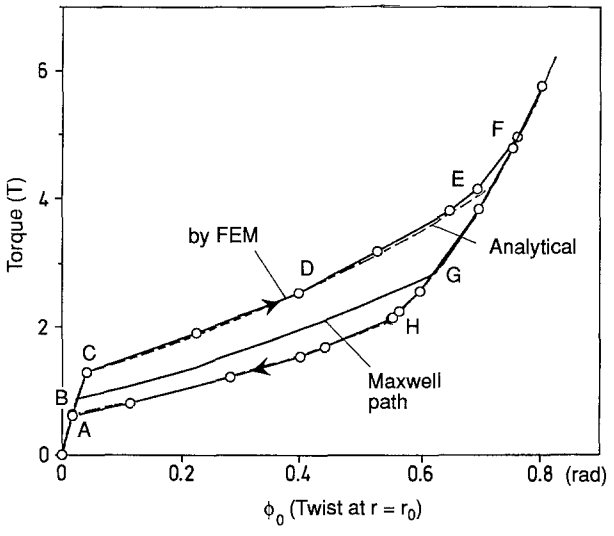

13

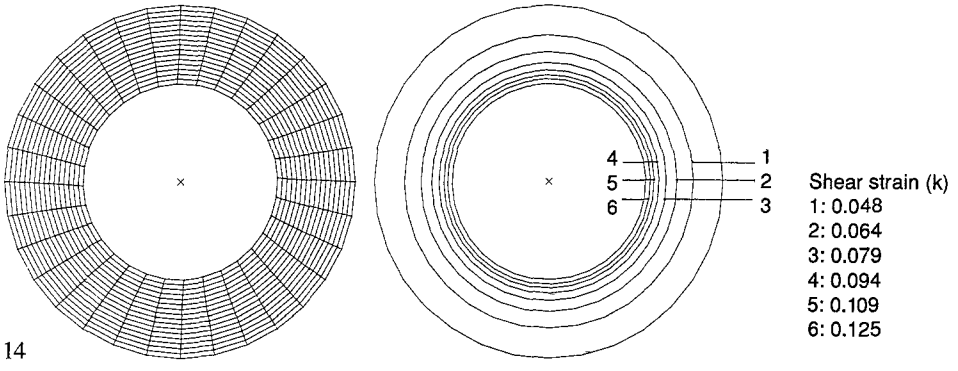

14

Figs. 13, 14. 13 The torque-twist curve of the tube problem. 14 Deformed mesh and shear strain distribution of the tube at state 'C'

Starting from the undeformed state 'O' ($T=0$), no shockline is observed up to the point 'C' ($T=2\pi(r_0)^2\tau_{max}$) in Fig. 13. The deformed configuration at 'C' is shown in Fig. 14. After passing point 'C', a shockline emerges at the inner surface and gradually moves outward (the path 'C'-'D'-'E' in Fig. 13). At point 'D', the shockline reaches the midpoint of inner and outer surfaces of the tube as shown in Fig. 15. At point 'E' ($T=2\pi(r_1)^2\tau_{max}$), the shockline reaches the outer surface retaining a smooth configuration, such as the state 'F', as shown in the Fig. 16. The shear strain distribution along r-direction between $[r_0, r_1]$ at states 'C', 'D', and 'F' is shown in Fig. 17. It can be seen that at state 'D', there is a gap $(k_1 \leftrightarrow k_3)$ in shear strain distribution corresponding to the shear stress τ_{max} on the shockline.

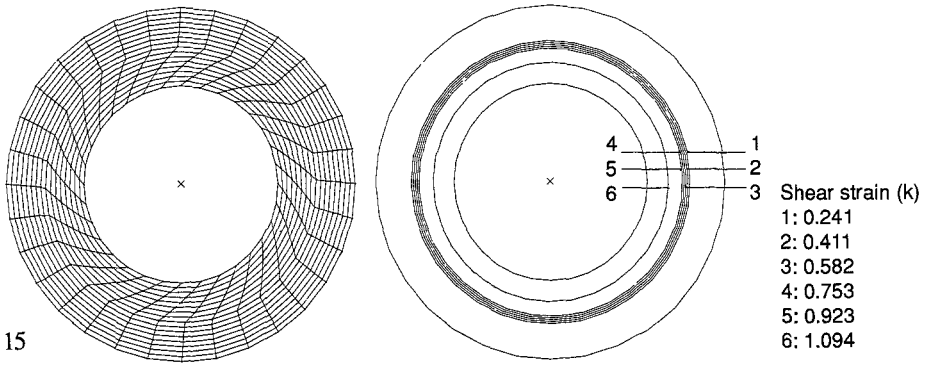

15

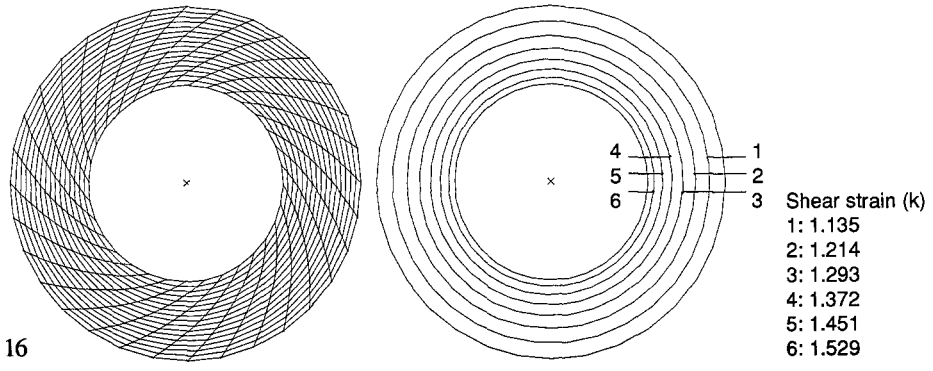

16

Figs. 15, 16. 15 Deformed mesh and shear strain distribution of the tube at state 'D'. 16 Deformed mesh and shear strain distribution of the tube at state 'F'

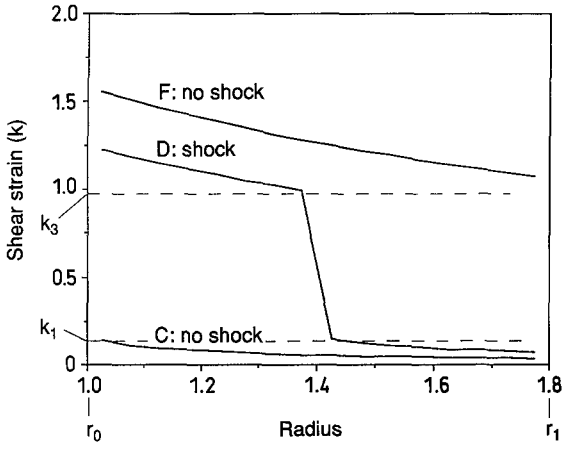

Fig. 17. Shear strain (k) distribution in the tube in radius direction at the states 'C', 'D', and 'F'

Then, we switch loading/unloading at the point 'F'. While unloading, we observe the process basically in reverse, whereas the shear stress on the shock is now τ_{min}. Hence, the solution does not take the same path after passing point 'E', and until point 'H', we observe smooth configurations. After passing 'H' ($T = 2\pi(r_1)^2\tau_{min}$), a shockline emerges at the outer surface and moves inward until it is absorbed by the inner surface at the point 'A' ($T = 2\pi(r_0)^2\tau_{min}$). Thus, we have a hysteresis loop A-B-C-D-E-F-G-H-A as shown in Fig. 15, and the area surrounded by the loop corresponds to the amount of the energy lost in one loading/unloading cycle. Therefore, the tube behaves as if it is composed of an elastic-plastic material when a shockline emerges.

5
Concluding remarks

In this paper, the formulation of the assumed stress hybrid elements for incompressible finite elasticity are presented. The formulations are derived directly from the discretized multi-field mixed variational principles involving complementary energy, with and without volume constraints. The variational

principles are modified by the regularization terms which enforce the angular momentum balance in the formulation. The suggested regularization forms are valid for not only linear but also nonlinear problems including finite rotation and stretching.

Two types of element formulation are presented. The first one has displacement (velocity), rotation (spin), and unsymmetric (Biot) stress as independent fields. In the second one, the hydrostatic pressure field is added as an independent field to account for volume constraints. In either formulation, each field is discretized using shape functions to construct four noded quadrilateral plane stress and plane strain elements which have C^0 continuous field, with displacement as nodal variables and the others as internal element variables. While assembling the mixed stiffness equation, stress parameters are eliminated at element level and only kinematic variables (for 'compressible' elements) or kinematic variables plus hydrostatic pressure (for 'incompressible' elements) remain in the mixed stiffness equation.

With minimum numbers of parameters, the elements pass the basic requirements such as desiable eigenvalues, patch tests and other benchmark tests in either linear or nonlinear cases. The performance of the elements is also checked by solving materially nonlinear problems, especially strain softening incompressible materials in which the ellipticity of the constitutive relation fails and discontinuous deformation gradient may occur.

As the first example of such a case, a block compression problem is analyzed. We observe the advent of shocklines between elliptic/hyperbolic materials and the formation of a shear band. The numerical results are compared with the semi-analytical methods and are in good agreement. The shear band thickness captured by the elements is reasonably small.

In the second example, the twisting of a tube, we observe a shockline of a different type between an elliptic material area and another elliptic area with a significant gap in shear strain but without shear band formation. We also observe that the solution path or shear stress on the shockline depends not only on the level of the load but also its path. In either case, the advent of the shocklines is confirmed by rapid changes or gaps in shear strain distribution by finite element analysis.

It is also found that the arclength method, in conjunction with the Newton-Raphson procedure, plays a crucial role analyzing these types of problems. As shown in the examples, the solution path may have snap-through problems and/or bifurcations, and in such a case, the simple load or displacement control method is no longer valid.

Appendix-I
Matrix forms of the discretized variational principles

We present the matrix form of the discretized principle in terms of $(\dot{\beta}^m, \omega^m, \dot{q}^m)$ for a single element (m-th element).

$$\dot{F}_{2.m}(\dot{\beta}^m, \omega^m, \dot{q}^m) = \frac{1}{2}\lfloor\dot{\beta}^m\rfloor[H^m_{\beta\beta}]\{\dot{\beta}^m\} + \frac{1}{2}\lfloor\omega^m\rfloor[G^m_{\omega\omega}]\{\omega^m\} + \lfloor\omega^m\rfloor[G^m_{\omega q}]\{\dot{q}^m\}$$

$$+\lfloor\dot{\beta}^m\rfloor[G^m_{\beta q}]\{\dot{q}^m\} + \lfloor\dot{\beta}^m\rfloor[G^m_{\beta\omega}]\{\omega^m\} - [\dot{Q}^m_q]\{\dot{q}^m\} \tag{A.1}$$

where

$$[H^m_{\beta\beta}] = -\int_{V_{N\,m}} [A_{\text{symm}}]^T[C][A_{\text{symm}}]\,dv$$

$$[G^m_{\omega\omega}] = -\int_{V_{N\,m}} [\Omega]^T\left(\frac{\tau_{11}+\tau_{22}}{2}\right)[\Omega]\,dv$$

$$[G^m_{\omega q}] = \int_{V_{N\,m}} [\Omega]^T[\hat{\tau}][B]\,dv$$

$$[G^m_{\beta q}] = \int_{V_{N.m}} [A]^T[B]\,dv$$

$$[G^m_{\beta\omega}] = -\int_{V_{N\,m}} [A_{\text{skew}}]^T[\Omega]\,dv$$

$$[\dot{Q}^m_q] = \int_{V_{N.m}} \rho^N[\dot{b}][B]\,dv + \int_{V_{N.m}\cap S_{\sigma N}} [\dot{\bar{T}}][B]\,dv \tag{A.2}$$

where $[C]$; the tangent compliance matrix defined by (93) or (94), $[\hat{\tau}]$ is a (4×4) matrix given by:

$$[\hat{\tau}] = \frac{1}{2}\begin{Bmatrix} 0 \\ -1 \\ 1 \\ 0 \end{Bmatrix} [-\tau_{12}\tau_{11} - \tau_{22}\tau_{21}] \tag{A.3}$$

and τ_{ij} are Cartesian components of τ^N.

The discretized regularization term (67) can be written by the following matrix forms as well:

$$-\frac{1}{2\gamma}\int_{V_N} |\mathrm{skew}(\dot{\mathbf{r}}^{*m} - \mathbf{W}^m \cdot \boldsymbol{\tau}^N + (\nabla^N \mathbf{v}^m)^N \cdot \boldsymbol{\tau}^N)|^2 \, dv$$

$$= \frac{1}{2}\lfloor \dot{\beta}^m \rfloor [H^{m,\gamma}_{\beta\beta}] \{\dot{\beta}^m\} + \frac{1}{2}\lfloor \omega^m \rfloor [G^{m,\gamma}_{\omega\omega}] \{\omega^m\} + \frac{1}{2}\lfloor \dot{q}^m \rfloor [G^{m,\gamma}_{qq}] \{\dot{q}^m\}$$

$$+ \lfloor \dot{\beta}^m \rfloor [G^{m,\gamma}_{\beta\omega}] \{\dot{\omega}^m\} + \lfloor \omega^m \rfloor [G^{m,\gamma}_{\omega q}] \{\dot{q}^m\} + \lfloor \dot{\beta}^m \rfloor [G^{m,\gamma}_{\beta q}] \{\dot{q}^m\} \tag{A.4}$$

where

$$[H^{m,\gamma}_{\beta\beta}] = -\gamma^{-1} \int_{V_{N\,m}} [A_{\mathrm{skew}}]^T [A_{\mathrm{skew}}] \, dv$$

$$[G^{m,\gamma}_{\omega\omega}] = -\gamma^{-1} \int_{V_{N,m}} [\Omega]^T \left(\frac{\tau_{11} + \tau_{22}}{2}\right)^2 [\Omega] \, dv$$

$$[G^{m,\gamma}_{qq}] = -\gamma^{-1} \int_{V_{N,m}} [B]^T [\hat{\tau}]^T [\hat{\tau}] [B] \, dv$$

$$[G^{m,\gamma}_{\beta\omega}] = \gamma^{-1} \int_{V_{N\,m}} [A_{\mathrm{skew}}]^T \left(\frac{\tau_{11} + \tau_{22}}{2}\right) [\Omega] \, dv$$

$$[G^{m,\gamma}_{\beta q}] = -\gamma^{-1} \int_{V_{N,m}} [A_{\mathrm{skew}}]^T [\hat{\tau}] [B] \, dv$$

$$[G^{m,\gamma}_{\omega q}] = \gamma^{-1} \int_{V_{N\,m}} [\Omega]^N \left(\frac{\tau_{11} + \tau_{22}}{2}\right) [\hat{\tau}] [B] \, dv. \tag{A.5}$$

The stationary condition of $\dot{F}_{2\gamma,m}(\dot{\beta}^m, \omega^m, \dot{q}^m)$ leads to the following system of equations:

$$\begin{bmatrix} H^{m*}_{\beta\beta} & G^{m*}_{\beta\omega} & G^{m*}_{\beta q} \\ G^{m*,T}_{\beta\omega} & G^{m*}_{\omega\omega} & G^{m*}_{\omega q} \\ G^{m*,T}_{\beta q} & G^{m*,T}_{\omega q} & G^{m*}_{qq} \end{bmatrix} \begin{Bmatrix} \dot{\beta}^m \\ \omega^m \\ \dot{q}^m \end{Bmatrix} = \begin{Bmatrix} 0 \\ 0 \\ \dot{Q}^m_q \end{Bmatrix} \tag{A.6}$$

where

$$[H^{m*}_{\beta\beta}] = [H^m_{\beta\beta}] + [H^{m,\gamma}_{\beta\beta}] \quad [G^{m*}_{\omega\omega}] = [G^m_{\omega\omega}] + [G^{m,\gamma}_{\omega\omega}]$$

$$[G^{m*}_{qq}] = [G^{m,\gamma}_{qq}] \qquad [G^{m*}_{\beta\omega}] = [G^m_{\beta\omega}] + [G^{m,\gamma}_{\beta\omega}]$$

$$[G^{m*}_{\beta q}] = [G^m_{\beta q}] + [G^{m,\gamma}_{\beta q}] \quad [G^{m*}_{\omega q}] = [G^m_{\omega q}] + [G^{m,\gamma}_{\omega q}]. \tag{A.7}$$

Likewise, for the four field formulation, we have the discretized form of a single element as follows:

$$\dot{G}_{2,m}(\dot{\beta}^m, \dot{p}^m, \omega^m, \dot{q}^m) = \frac{1}{2}\lfloor\dot{\beta}^m\rfloor[H^m_{\beta\beta}]\{\dot{\beta}^m\} + \lfloor\dot{\beta}^m\rfloor[H^m_{\beta p}]\dot{p}^m + \frac{1}{2}\dot{p}^m[H^m_{pp}]\dot{p}^m$$

$$+\frac{1}{2}\lfloor\dot{\omega}^m\rfloor[G^m_{\omega\omega}]\{\omega^m\} + \lfloor\omega^m\rfloor[G^m_{\omega q}]\{\dot{q}^m\} + \lfloor\dot{\beta}^m\rfloor[G^m_{\beta q}]\{\dot{q}^m\}$$

$$+\dot{p}^m[G^m_{pq}]\{\dot{q}^m\} + \lfloor\dot{\beta}^m\rfloor[G^m_{\beta\omega}]\{\omega^m\} - [\dot{Q}^m_q]\{\dot{q}^m\} \tag{A.8}$$

where

$$[H^m_{\beta\beta}] = -\int_{V_{N\,m}} [\bar{A}_{\text{symm}}]^T[C_{rr}][\bar{A}_{\text{symm}}]\,dv$$

$$[H^m_{\beta p}] = -\int_{V_{N,m}} [\bar{A}_{\text{symm}}]^T[C_{rp}][P]\,dv$$

$$[H^m_{pp}] = -\int_{V_{N,m}} [P]^T(C_{pp})[P]\,dv$$

$$[G^m_{\omega\omega}] = -\int_{V_{N,m}} [\Omega]^T\left(\frac{\tau_{11}+\tau_{22}}{2}\right)[\Omega]\,dv$$

$$[G^m_{\omega q}] = \int_{V_{N,m}} [\Omega]^T[\hat{\tau}][B]\,dv$$

$$[G^m_{\beta q}] = \int_{V_{N\,m}} [\bar{A}]^T[\bar{B}]\,dv$$

$$[G^m_{pq}] = \int_{V_{N\,m}} [P]^T[B_v]\,dv$$

$$[G^m_{\beta\omega}] = -\int_{V_{N,m}} [A_{\text{skew}}]^T[\Omega]\,dv$$

$$[Q^m_q] = \int_{V_{N,m}} \rho^N\lfloor\dot{b}\rfloor[B]\,dv + \int_{\partial V_{N\,m}\cap S_{\sigma N}} \lfloor\dot{\bar{T}}\rfloor[B]\,dv \tag{A.9}$$

where $[C_{rr}]$, $[C_{rp}]$, (C_{pp}) are the coefficient matrices in the following rate constitutive relations:

$$\dot{W}_c(\text{symm}\,\dot{\mathbf{r}}^{*'}, \dot{p}) = \frac{1}{2}\lfloor\text{symm}\,\dot{r}^{*'}_{ij}\rfloor[C_{rr}]\{\text{symm}\,\dot{r}^{*'}_{ij}\} + [\text{symm}\,\dot{r}^{*'}_{ij}][C_{rp}]\dot{p} + \frac{1}{2}\dot{p}\,C_{pp}\dot{p}. \tag{A.10}$$

The form (A.4) can also be used for the regularization of the four field formulation since the same shape function is used for $\mathbf{r}^*$ and $\mathbf{r}^{*'}$. Likewise, we have a equation system:

$$\begin{bmatrix} H^{m*}_{\beta\beta} & H^m_{\beta p} & G^{m*}_{\beta\omega} & G^{m*}_{\beta q} \\ H^{m,T}_{\beta p} & H^m_{pp} & 0 & G^m_{pq} \\ G^{m*,T}_{\beta\omega} & 0 & G^{m*}_{\omega\omega} & G^{m*}_{\omega q} \\ G^{m*,T}_{\beta q} & G^{m,T}_{pq} & G^{m*,T}_{\omega q} & G^{m*}_{qq} \end{bmatrix} \begin{Bmatrix} \dot{\beta}^m \\ \dot{p}^m \\ \omega^m \\ \dot{q}^m \end{Bmatrix} = \begin{Bmatrix} 0 \\ 0 \\ 0 \\ \dot{Q}^m_q \end{Bmatrix} \tag{A.11}$$

where $[H^{m*}_{\beta\beta}]$, $[G^{m*}_{\beta\omega}]$, $[G^{m*}_{\beta q}]$, $[G^{m*}_{\omega q}]$, $[G^{m*}_{qq}]$ are given by (A.7) since the common shape function is used for $\mathbf{r}^*$ and $\mathbf{r}^{*'}$.

Appendix-II
Stiffness matrices by eliminating β

By eliminating β, the single element stiffness equation for the three field formulation is reduced to:

$$\begin{bmatrix} K^m_{\omega\omega} & K^m_{\omega q} \\ K^{m,T}_{q\omega} & K^m_{qq} \end{bmatrix} \begin{Bmatrix} \omega^m \\ \dot{q}^m \end{Bmatrix} = \begin{Bmatrix} 0 \\ \dot{Q}^m_q \end{Bmatrix} \tag{A.12}$$

where

$$[K^m_{\omega\omega}] = [G^{m*}_{\omega\omega}] - [G^{m*}_{\beta\omega}]^T [H^{m*}_{\beta\beta}]^{-1} [G^{m*}_{\beta\omega}]$$

$$[K^m_{\omega q}] = [G^{m*}_{\omega q}] - [G^{m*}_{\beta\omega}]^T [H^{m*}_{\beta\beta}]^{-1} [G^{m*}_{\beta q}]$$

$$[K^m_{qq}] = [G^{m*}_{qq}] - [G^{m*}_{\beta q}]^T [H^{m*}_{\beta\beta}]^{-1} [G^{m*}_{\beta q}] \tag{A.13}$$

and $\dot{\beta}$ can be found by solving (A.12):

$$\{\dot{\beta}\} = -[H^{m*}_{\beta\beta}]^{-1} ([G^{m*}_{\beta\omega}]\{\omega^m\} + [G^{m*}_{\beta q}]\{\dot{q}\}). \tag{A.14}$$

For the four field formulation:

$$\begin{bmatrix} K^m_{pp} & K^m_{p\omega} & K^m_{pq} \\ K^{m,T}_{p\omega} & K^m_{\omega\omega} & K^m_{\omega q} \\ K^{m,T}_{pq} & K^{m,T}_{\omega q} & K^m_{qq} \end{bmatrix} \begin{Bmatrix} \dot{p}^m \\ \omega^m \\ \dot{q}^m \end{Bmatrix} = \begin{Bmatrix} 0 \\ 0 \\ \dot{Q}^m_q \end{Bmatrix} \tag{A.15}$$

where

$$[K^m_{pp}] = [H^m_{pp}] - [G^{m*}_{\beta p}]^T [H^{m*}_{\beta\beta}]^{-1} [G^{m*}_{\beta p}]$$

$$[K^m_{p\omega}] = [G^m_{p\omega}] - [G^{m*}_{\beta p}]^T [H^{m*}_{\beta\beta}]^{-1} [G^{m*}_{\beta\omega}]$$

$$[K^m_{pq}] = [G^m_{pq}] - [G^{m*}_{\beta p}]^T [H^{m*}_{\beta\beta}]^{-1} [G^{m*}_{\beta q}] \tag{A.16}$$

$K^m_{\omega\omega}$, $K^m_{\omega q}$, and K^m_{qq} are given by the same form as (A.13).

Appendix-III
Newton-Raphson method

Denote Δt as the time difference between C_N and C_{N+1}. We impose boundary conditions (including body forces) so that $\dot{Q}^m_q$ in (A.2) is constant during Δt. By solving (A.6) for $(\dot{\beta}, \omega, \dot{q})$ or (A.11) for $(\dot{\beta}, \dot{p}, \omega, \dot{q})$, we find the rates using the shape functions:

$$\{v_{i.j}\} = [B]\{\dot{q}^m\}, \quad \{W_{ij}\} = [\Omega]\{\omega^m\}, \quad \{\dot{r}^*_{ij}\} = [A]\{\dot{\beta}^m\}$$

or in the four field formulation,

$$\{\dot{r}^{*'}_{ij}\} = [A]\{\dot{\beta}^m\}, \quad \dot{p} = [P]\{\dot{q}^m\}. \tag{A.17}$$

The field variables at C_{N+1} state are updated as:

$$\mathbf{u}^{N+1} = \mathbf{u}^N + \Delta t \mathbf{v}$$

$$\mathbf{R}^{N+1} = \mathbf{R}^N + \Delta t \mathbf{W}$$

$$\mathbf{r}^{*N+1} = \mathbf{r}^{*N} + \Delta t \dot{\mathbf{r}}^*$$

or in the four field formulation,

$$\mathbf{r}^{*'N+1} = \mathbf{r}^{*'N} + \Delta t \dot{\mathbf{r}}^{*'}, \quad p^{N+1} = p^N + \Delta t \dot{p}. \tag{A.18}$$

The first Piola-Kirchhoff stress can be found from (A.18):

$$\mathbf{t}^{N+1} = \boldsymbol{\tau}^N + \Delta t[\dot{\mathbf{r}}^* - \boldsymbol{\tau}^N \cdot \mathbf{W}]. \tag{A.19}$$

Note that since UL description is adopted, we have $\mathbf{u}^N = \mathbf{0}$, $\mathbf{R}^N = \mathbf{I}$, $\mathbf{r}^{*N} = \boldsymbol{\tau}^N$.

Since a finite value is taken for Δt, there are mismatches that need to be corrected in the above numerical procedure. In three field formulation, the residuals in the constitutive relation, AMB, and LMB are denoted by $\lfloor \dot{R}_\beta \rfloor \{\dot{\beta}\}$, $\lfloor \dot{R}_\omega \rfloor \{\omega\}$, and $\lfloor \dot{R}_q \rfloor \{\dot{q}\}$:

$$\{\dot{R}_\beta^m\} = (\Delta t)^{-1} \int_{V_{Nm}} [A]^T \left\{ \left(\frac{\partial W_c(\operatorname{symm} \mathbf{r}^*)}{\partial (\mathbf{r}^*)^T} \right)^{N+1} - (\mathbf{R}^{N+1})^T \cdot (\mathbf{I} + \nabla^N \mathbf{u}^{N+1})^T \right\}_{\alpha\beta} dv$$

$$\{\dot{R}_\omega^m\} = (\Delta t)^{-1} \int_{V_{N,m}} [\Omega]^T \{ \operatorname{skew}[(\mathbf{R}^{N+1})^T \cdot (\mathbf{I} + \nabla^N \mathbf{u}^{N+1})^T \cdot \mathbf{r}^{*N+1}] \}_{\alpha\beta} dv$$

$$\{\dot{R}_q^m\} = (\Delta t)^{-1} \int_{V_{Nm}} [B]^T \{ \mathbf{r}^{*N+1} \cdot (\mathbf{R}^{N+1})^T - \tau^N \}_{\alpha\beta} dv \tag{A.20}$$

where $\{\}_{\alpha\beta}$ means $\lfloor ()_{1,1}\ ()_{1,2}\ ()_{2,1}\ ()_{2,2} \rfloor^T$.

Then, we have a system of equations for correction terms.

$$\begin{bmatrix} H_{\beta\beta}^{m*} & G_{\beta\omega}^{m*} & G_{\beta q}^{m*} \\ G_{\beta\omega}^{m*,T} & G_{\omega\omega}^{m*} & G_{\omega q}^{m*} \\ G_{\beta q}^{m*,T} & G_{\omega q}^{m*,T} & G_{qq}^{m*} \end{bmatrix} \begin{Bmatrix} \Delta\dot{\beta}^m \\ \Delta\omega^m \\ \Delta\dot{q}^m \end{Bmatrix} = \begin{Bmatrix} 0 \\ 0 \\ \dot{Q}_q^m \end{Bmatrix} - \begin{Bmatrix} \dot{R}_\beta^m \\ \dot{R}_\omega^m \\ \dot{R}_q^m \end{Bmatrix}. \tag{A.21}$$

For simplicity, we denote the variables collectively as:

$$[K] = \begin{bmatrix} H_{\beta\beta}^{m*} & G_{\beta\omega}^{m*} & G_{\beta q}^{m*} \\ G_{\beta\omega}^{m*,T} & G_{\omega\omega}^{m*} & G_{\omega q}^{m*} \\ G_{\beta q}^{m*,T} & G_{\omega q}^{m*,T} & G_{qq}^{m*} \end{bmatrix}, \quad \{\Delta x\} = \begin{Bmatrix} \Delta\dot{\beta}^m \\ \Delta\omega^m \\ \Delta\dot{q}^m \end{Bmatrix}, \quad \{Q\} = \begin{Bmatrix} 0 \\ 0 \\ \dot{Q}_q^m \end{Bmatrix}, \quad \{R\} = \begin{Bmatrix} \dot{R}_\beta^m \\ \dot{R}_\omega^m \\ \dot{R}_q^m \end{Bmatrix}. \tag{A.22}$$

Then, the standard Newton-Raphson procedure is written as:

$$\{x^{k+1}\} - \{x^k\} = \{\Delta x\} = [K^k]^{-1}(\{Q^k\} - \{R^k\}) \tag{A.23}$$

where k denotes the k-th iteration. After each iteration, we correct parameters ($\dot{\beta} \leftarrow \dot{\beta} + \Delta\dot{\beta}, \ldots$) and go back to (A.17), (A.18) to update field variables and recalculate the residual terms. The process is repeated until certain convergence conditions ($|\Delta x| = |x^{k+1} - x^k| <$ tolerance and/or $|Q^k - R^k| <$ tolerance) are satisfied.

For the four field formulation, we have the following residual terms:

$$\{\dot{R}_\beta^m\} = (\Delta t)^{-1} \int_{V_{Nm}} [\bar{A}]^T \left\{ \left(\frac{\partial W_c'(\operatorname{symm} \mathbf{r}^{*'}, p)}{\partial (\mathbf{r}^{*'})^T} \right)^{N+1} - (\mathbf{R}^{N+1})^T \cdot (\mathbf{I} + \nabla^N \mathbf{u}^{N+1})^T (J_{\mathrm{u,R}}^{N+1})^{-1/3} \right\}_{ij} dv$$

$$\{\dot{R}_\omega^m\} = (\Delta t)^{-1} \int_{V_{Nm}} [P]^T \left\{ \left(\frac{\partial W_c'(\operatorname{symm} \mathbf{r}^{*'}, p)}{\partial p} \right)^{N+1} - f(J_{\mathrm{u,R}}^{N+1}) \right\}_{ij} dv$$

$$\{\dot{R}_\omega^m\} = (\Delta t)^{-1} \int_{V_{N,m}} [\Omega]^T \{ \operatorname{skew}[(\mathbf{R}^{N+1})^T \cdot (\mathbf{I} + \nabla^N \mathbf{u}^{N+1})^T \cdot \mathbf{r}^{*'N+1}] \}_{\alpha\beta} dv$$

$$\{\dot{R}_\omega^m\} = (\Delta t)^{-1} \int_{V_{N,m}} [\bar{B}]^T \Big\{ \mathbf{r}^{*'N+1} \cdot (\mathbf{R}^{N+1})^T (J_{\mathrm{u,R}}^{N+1})^{-1/3}$$

$$- \frac{1}{3} [\mathbf{r}^{*'N+1} : ((\mathbf{I} + \nabla^N \mathbf{u}^{N+1}) \cdot \mathbf{R}^{N+1})(J_{\mathrm{u,R}}^{N+1})^{-1/3}] (\mathbf{I} + \nabla^N \mathbf{u}^{N+1})^{-T}$$

$$+ p^{N+1} f'(J_{\mathrm{u,R}}^{N+1}) J_{\mathrm{u,R}}^{N+1} (\mathbf{I} + \nabla^N \mathbf{u}^{N+1})^{-T} - \tau^N \Big\}_{\alpha\beta} dv \tag{A.24}$$

where $\{\}_{ij}$ means $\lfloor ()_{1,1}\ ()_{1,2}\ ()_{2,1}\ ()_{2,2}\ ()_{3,3} \rfloor^T$.

Thus, the equations for the correction terms are:

$$\begin{bmatrix} H^{m*}_{\beta\beta} & H^{m}_{\beta p} & G^{m*}_{\beta\omega} & G^{m*}_{\beta q} \\ H^{m,T}_{\beta p} & H^{m}_{pp} & 0 & G^{m}_{pq} \\ G^{m*,T}_{\beta\omega} & 0 & G^{m*}_{\omega\omega} & G^{m*}_{\omega q} \\ G^{m*,T}_{\beta q} & G^{m,T}_{pq} & G^{m*,T}_{\omega q} & G^{m*}_{qq} \end{bmatrix} \begin{Bmatrix} \Delta\dot{\beta}^m \\ \Delta\dot{p}^m \\ \Delta\dot{\omega}^m \\ \Delta\dot{q}^m \end{Bmatrix} = \begin{Bmatrix} 0 \\ 0 \\ 0 \\ \dot{Q}^m_q \end{Bmatrix} - \begin{Bmatrix} \dot{R}^m_\beta \\ \dot{R}^m_p \\ \dot{R}^m_\omega \\ \dot{R}^m_q \end{Bmatrix}. \tag{A.25}$$

The Newton-Raphson procedure is the same as (A.23).

References

Abeyaratne, R. 1981: Discontinuous deformation gradients in the finite twisting of an incompressible elastic tube. J. Elasticity 11: 43–80

Abeyaratne, R.; Yang, J. S. 1987: Localized shear discontinuities near the tip of a mode I crack. J. Elasticity 17: 93–112

Abeyaratne, R.; Knowles, J. K. 1987: Non-elliptic elastic materials and the modeling of dissipative mechanical behavior: an example. J. Elasticity 18: 227–278

Abeyaratne, R.; Knowles, J. K. 1989: Equilibrium shocks in plane deformation of incompressible elastic materials. J. Elasticity 22: 63–80

Allman, D. J. 1984: A compatible triangular element including vertex rotations for plane elasticity analysis. Comput. Struct. 19: 1–8

Atluri, S. N. 1973: On the hybrid stress finite element model in incremental analysis of large deflection problems. Int. J. Solids Struct. 9: 1188–1191

Atluri, S. N.; Murakawa, H. 1977: Hybrid finite element models in nonlinear solid mechanics. In: Bergan, P. G. et al. (eds.) On hybrid finite element models in nonlinear solid mechanics. Finite elements in Nonlinear Mechanics, vol. 1, pp. 3–41. Norway: Tapir Press

Atluri, S. N. 1980: On some new general and complementary energy theorems for the rate problems in finite strain, classical elastoplasticity. J. Struct. Mech. 8: 61–92

Atluri, S. N. 1984: Alternate stress and conjugate strain measures, and mixed variational formulations involving rigid rotations, for computational analyses of finitely deformed solids, with application to plates and shells—I Theory. Comput. Struct. 18: 98–116

Atluri, S. N.; Reissner, E. 1989: On the formulation of variational theorems involving volume constraints. Comput. Mech. 5: 337–344

Batra, R. C.; Ko, K. I. 1992: An adaptive mesh refinement technique for the analysis shear bands in plane strain compression of a thermoviscoplastic solid. Comput. Mech. 10: 369–379

Belytschko, T.; Fish, J.; Engelmann, B. E. 1988: A finite element with embedded localization zones. Comput. Methods Appl. Mech. and Engng. 70: 59–89

Cazzani, A.; Atluri, S. N. 1993: Four-noded mixed finite elements, using unsymmetric stresses, for linear analysis of membranes. Comput. Mech. 11: 229–251

Chrisfield, M. A. 1983: An arc-length method including line searches and acceleration. Inter. J. Num. Methods Engng. 19: 1269–1289

Cook, R. D. 1974: Improved two dimensional finite elements. ASCE Structural Division Journal ST6: 1851–1863

Hughes, T. J. R.; Brezzi, R. 1989: On drilling degrees of freedom. Comput. Methods Appl. Mech. Engng. 72: 105–121

Ibrahimbegovic, A. 1993: Mixed finite element with drilling rotations for plane problems in finite elasticity. Comput. Methods Appl. Mech. Engng. 107: 225–238

Iura, M.; Atluri, S. N. 1992: Formulation of a membrane finite element with drilling degrees of freedom. Comput. Mech. 9: 417–428

Kondoh, K.; Atluri, S. N. 1985: Influence of local buckling on global instability: Simplified, large deformation, post-bukling analyses of plane trusses. Comput. Struct. 21: 613–627

Murakawa, H.; Atluri, S. N. 1978: Finite elasticity solutions using hybrid finite elements based on a complementary energy principle. ASME J. Appl. Mech. 45: 539–547

Murakawa, H.; Atluri, S. N. 1979: Finite elasticity solutions using hybrid finite elements based on a complementary energy principle. Part 2: Incompressible materials. ASME J. Appl. Mech. 46: 71–77

Oden, J. T.; Kikuchi, N.; Song, Y. J. 1982: Penalty-finite element methods for the analysis of Stokesian flows. Comput. Methods Appl. Mech. Engng. 31: 297–329

Oden, J. T.; Jacquotte, O. P. 1984: Stability of some mixed finite element methods for Stokesian flows. Comput. Methods Appl. Mech. Engng. 43: 231–248

Ortiz, M.; Leroy, Y.; Needleman, A. 1987: A finite element method for localized failure analysis. Comput. Methods Appl. Mech. Engng. 61: 189–214

Pian, T. H. H. 1964: Derivation of element stiffness matrices by assumed stresses and displacements. AIAA Journal 2: 1333–1336

Pian, T. H. H.; Sumihara, K. 1984: Rational approach for assumed stress finite elements. Int. J. Num. Methods Engng. 20: 1685–1695

Pian, T. H. H.; Wu, C. C. 1988: A rational approach for choosing stress terms for hybrid finite element formulations. Inter. J. Num. Methods Engng. 26: 2331–2343

Punch, E. F.; Atluri, S. N. 1984: Development and testing of stable, invariant, isoparametric curvilinear 2- and 3-D hybrid stress elements. Comput. Methods Appl. Mech. Engng. 47: 331–356

Reed, K. W.; Atluri, S. N. 1983: Analyses of large quasistatic deformations of inelastic bodies by a new hybrid-stress finite element algorithm. Comput. Methods Appl. Mech. Engng. 39: 245–295

Riks, E. 1972: The application of Newton's method to the problem of elastic stability. J. Appl. Mech. 39: 1060–1066
Rubinstein, R.; Punch, E. F.; Atluri, S. N. 1983: An analysis of, and remedies for, kinematic modes in hybrid-stress finite elements: selection of stable, invariant stress fields. Comput. Methods Appl. Mech. Engng. 38: 63–92
Simo, J. C.; Fox, D. D.; Hughes, T. J. R. 1992: Formulations of finite elasticity with independent rotations. Comput. Methods Appl. Mech. Engng. 95: 277–288
Timoshenko, S.; Goodier, J. N. 1970: Theory of elasticity, 3rd ed. New York: McGraw-Hill
Washizu, K. 1982: Variational methods in elasticity and plasticity, 3rd ed. Oxford: Pergamon Press
Xue, W. M.; Karlovitz, L. A.; Atluri, S. N. 1985: On the existence and stability conditions for mixed-hybrid finite solutions based on Reissner's variational principle. Inter. J. Solids and Structures 21(1): 97–116
Ying, L. A.; Atluri, S. N. 1983: A hybrid finite element method for Stokes flow: Part II—Stability and convergence studies. Comput. Methods Appl. Mech. Engng. 36: 39–60